COMPUTER AIDED METHODS FOR ASSISTING COCHLEAR IMPLANT SURGERY

PhD Thesis

Bence Horváth, MSc
University of Szeged, Faculty of Medicine
Szent-Györgyi Albert Clinical Center, Department of Otorhinolaryngology, Head and Neck Surgery

Supervisor:
József Géza Kiss, CSc, PhD
Co-supervisor:
Ádám Perényi, MD, PhD

Doctoral School of Clinical Medicine
Chair: Prof. Lajos Kemény MD, DSc

Szeged
2022

PUBLICATIONS RELATED TO THE THESIS:

I. **Horváth Bence**, Nagy Attila, Beöthy-Fehér Orsolya, Rovó , Kiss József Géza, Az emberi hibatényező vizsgálata CT felvételek manuális kiértékelésekor, A XXXI. Neumann Kollokvium konferencia-kiadványa, 2018 Szeged, ISBN: 978-615-503-614-9.

II. **Horváth B**, Perényi Á, Molnár AF, Csanády M, Kiss GJ, Rovó L. A new method to determine the optimal orientation of Slim Modiolar cochlear implant electrode array insertion. Ideggyogy Sz. 2021 May 30;74(5-6):191-195. English. doi: 10.18071/isz.74.0191. PMID: 34106549.
Impact factor: **0.708**

III. **Horváth B**, Perényi Á, Molnár AF, Csanády M, Kiss GJ, Rovó L. A new method of pre-operative assessment of correct electrode array alignment based on post-operative measurements in a cochlear implanted cohort. European Archives of Oto-Rhino-Laryngology. 2022
Impact factor: **3.236**

IV. Perényi Á, Nagy R, **Horváth B**, Posta B, Dimák B, Csanády M, Kiss JG, Rovó L. Új műtéti képalkotó lehetőség a belsőfül-implantátum elektródasorának dinamikus helyzetmeghatározására [A novel intraoperative imaging tool to follow the cochlear implant electrode array insertion dynamics]. Orv Hetil. 2021 May 30;162(22):878-883. Hungarian. doi: 10.1556/650.2021.32085. PMID: 34052802.
Impact factor: **0.707**

PUBLICATIONS NOT DIRECTLY RELATED TO THE PHD THESIS:

I. **Horváth B**, Ormos P, Kelemen L. Nearly Aberration-Free Multiphoton Polymerization into Thick Photoresist Layers. Micromachines (Basel). 2017 Jul 13;8(7):219. doi: 10.3390/mi8070219. PMID: 30400410; PMCID: PMC6190196.
Impact factor: 2.222

II. Kelemen L, Lepera E, **Horváth B**, Ormos P, Osellame R, Martínez Vázquez R. Direct writing of optical microresonators in a lab-on-a-chip for label-free biosensing. Lab Chip. 2019 Jun 7;19(11):1985-1990. doi: 10.1039/c9lc00174c. Epub 2019 May 2. PMID: 31044200.
Impact factor: 6.774

III. **Horváth Bence**, Nagy Attila, Beöthy-Fehér Orsolya, Rovó László, Kiss József Géza, Felhasználók szubjektivitásának vizsgálata CT-felvételek kiértékeléséből származó adatok elemzésével, FÜL-ORR-GÉGEGYÓGYÁSZAT (0016-237X): 64 3 pp 99-99 (2018)

Impact factor related to the thesis: **4.651**
Cumulative impact factor: **13.647**

COOPERATION

1. Department of Radiology, Albert Szent-Györgyi Clinical Center, University of Szeged
2. 3D (Printing) Center of the University of Szeged
3. Cochlear Ltd, Sydney, Australia
4. MED-EL GmbH, Innsbruck, Austria

ABBREVIATIONS

CI	Cochlear Implant
CT	Computed Tomography
EA	Electrode Array
FL	Fluoroscopy
IG	Insertion Guide
ISP	Incus Short Process
MRI	Magnetic Resonance imaging
OM	Orientation Marker
PEA	Perimodiolar Electrode Array
[ref.]	Self-citation from published manuscript
RW	Round Window
SEA	Straight Electrode Array
SM	Slim Modiolar electrode array
TFO	Tip Fold-Over

TABLE OF CONTENT

I. INTRODUCTION

As one of our most important senses, the ability to hear enables us to connect to the world for many very important, even vital, reasons. Most importantly, hearing connects us to people enabling us to communicate in a way that none of our other senses can achieve. First of all, prelingual hearing impaired people born as or become profoundly hearing impaired at a young age, which condition maintained before the period of speech development. These are the patients, who if completely lack the experience of hearing, would never learn to speak. To prevent this, regardless of age the hearing should be restored as soon as possible [1], to avoid the deterioration of quality of life (work, human relations etc.) [2]. However, thanks to advanced equipment and surgical techniques, they have the opportunity to hear. Our research focuses on the use of cochlear implants, which are the most modern implantable devices of the inner ear.

I.1. Cochlear implant (CI)

The history of cochlear implantation technology can be traced back to the 18th century. Alessandro Volta was the first, who carried out research in 1790 with electrical stimulation of hearing [3]. The cochlear implant directly stimulates the auditory nerve, which creates a hearing experience for the patient [4]. This means that the device takes over the role of the inner hair-cells. The first direct electrical stimulation of the auditory nerve occurred in the 1950s by Andre Djourno and Charles Eyries [5].

The implant consists of two main units (Figure 1. [6]). The internal unit contains the electrode array (EA) which is surgically inserted into the scala tympani of the cochlea. The most common procedure to insert EA into the scala tympani via the round window (RW) is a partial mastoidectomy followed by a posterior tympanotomy [7]. The RW anatomy is variable among individuals [8] which in some instances requires its widening ("extended RW approach" [9]). The electrode is placed near to the auditory nerve, so the nerve undergoes directs stimulation. For this reason, maintaining the integrity of the auditory nerve is essential. The other end of the electrode terminates in a transmitter/receiver unit that is implanted under the scalp. This system converts the sound that is captured by the outer unit into electrical impulses.

The external unit includes a microphone that captures the sounds of the environment and transmits these sounds to the speech processor. The external and internal units are connected by a magnet through the scalp. To achieve the best hearing experience, the device should be calibrated at least once a week and then once a month after implantation. At this time, the calibration technician will fine-tune the set parameters of the device based on the patient's feedback [10].

There are two main EA types, straight and precurved electrode arrays. These are described in the following sections.

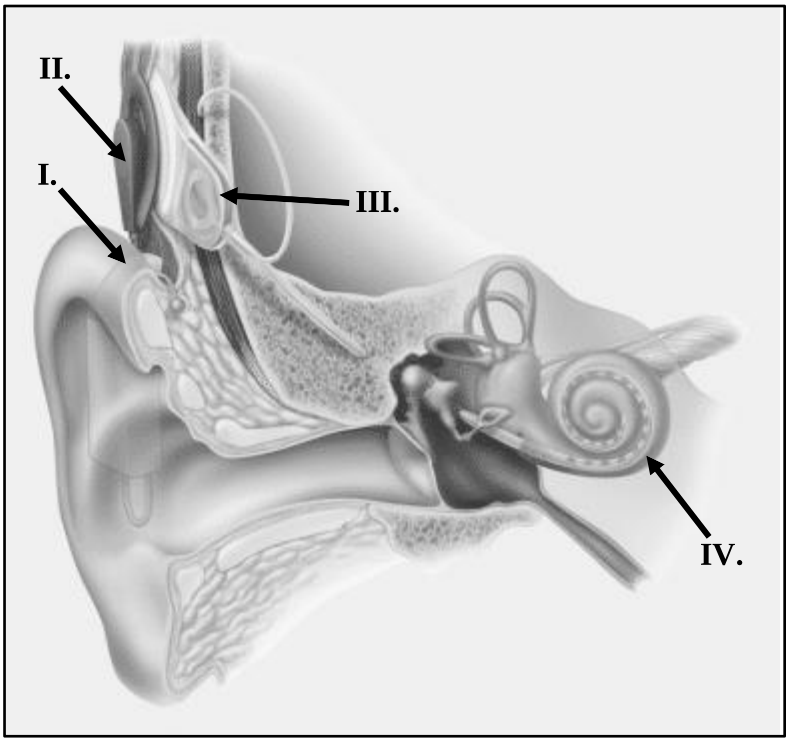

Figure 1. The placement of the Cochlear implant and its parts illustrating on the right ear. The components of the external unit: microphone (I.), which is located behind the ear. The speech processor (II.), which is connected with the transmitter (III.) through the scalp by a magnet. Inside the inner ear the electrode array implanted into the cochlear duct (IV.)

I.1.1. <u>Cochlear implant electrode arrays</u>

The cochlear implant EA dimensions should be matched to the size of the cochlea, when choosing the EA for a given patient. The average length of the cochlear duct is approximately 35 mm [11, 12], and the diameter of the basal turn measures approximately 2 mm. CI companies designed the EAs by different philosophy [13, 14]. Med-El® construct their EAs with different lengths from 31.5 mm (STANDARD) to 15 mm (COMPRESSED), to achieve EA's full insertion into the cochlear duct. According to Cochlear™ Ltd. full insertion is not necessary and only cover the basal turn of the cochlea is enough.

I.1.1.1 Straight electrode array (SEA)

SEAs have been designed by multiple CI manufacturers (Cochlear™ Ltd., Med-El® etc.). The long lifetime and the large number of implanted devices [15, 16] show the clinical efficacy and reliability of SEAs. These EAs are located near to the lateral wall of the cochlea. SEAs have also been used in a significant proportion of patients with different anatomical variations, particularly when the cochlear structure is not suitable for perimodiolar electrode placement [17, 18] . The Slim Straight electrode with the Nucleus® CI422 and CI522 electrodes has been shown in numerous studies [19] to be suitable for long-term low frequency hearing preservation.

Figure 2. Illustration of the main types of CI electrode arrays design. a) Slim straight electrode, b) Precurved Slim Modiolar, electrode. These presented electrode arrays are manufactured by Cochlear™ Ltd. .

I.1.1.2 Perimodiolar electrode array (PEA)

The scientific foundations of perimodiolar placement were established by Shepherd et al. [20]. PEAs have been designed to be placed near to the modiolus of the cochlea therefore, the electrodes are in closer proximity to the auditory nerve than the straight EA. There are many positive effects, such as the stimulation takes place closer to the auditory nerve, which can be reflected in both more effective electrophysiological parameters and improved hearing experience. The PEA begins to take on the twisted shape of the cochlea as soon as it leaves the EA insertion tool which can reduce the risk of any damage to the cochlea's inner structures. This can be justified by better hearing preservation. PEAs (CI532 and CI632 from the Cochlear™ Ltd.) have been the most commonly used electrode arrays for patients who experienced severe to profound sensorineural hearing loss at our Department.

Besides the many advantages of the delicate EA, it has a significant draw-back: tip fold-over (TFO), when the EA is turned back inside the cochlear duct [21, 22]. This phenomenon should be avoided because it can cause implant failure and a need for removal. An example of TFO is shown on Figure 3.

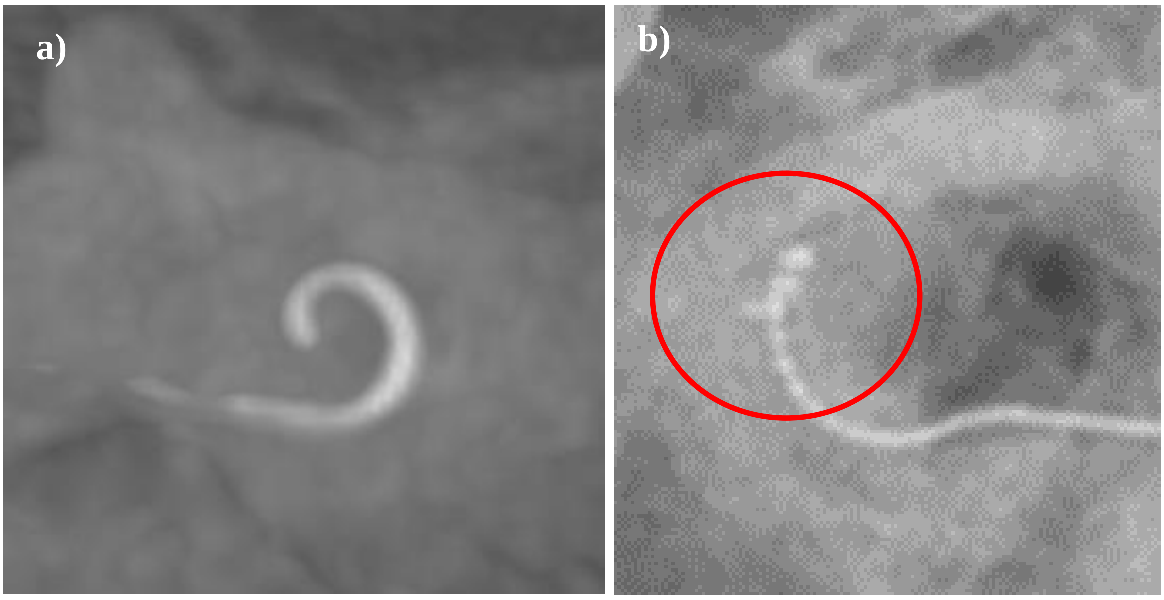

Figure 3. Post operative CT scans for two CI cases at our Department. ***a)*** *Successfully implantation case at the left cochlea. The EA was fully inserted into the cochlear duct,* ***b)*** *A failed implantation inside the right cochlea: tip fold-over occurred. The electrode array twisted and turned back inside the cochlea thus the array had to be removed and reimplantation was attempted.*

I.1.1.3 Half-banded and full-banded EAs

In the half-banded EAs [23], the electrode contact points are located only in the half part of the silicon coat's cross-section. The half-banded design enables the electrode insertion direction critical, because it can only twist in one direction. This is unlike the full-banded electrodes, where the electrodes fill the entire cross-section of the silicone case. For this reason, half-banded EA's insertion tool is equipped with an orientation marker (OM) to align the implant to the correct trajectory.

I.2. Medical imaging

In line with the international guidelines, our patients who are candidates for cochlear implantation, undergo imaging with Computed Tomography (CT) and/or Magnetic Resonance Imaging (MRI) [24].

Pre-operative imaging is essential to diagnose any type of inner ear malformations and to identify other abnormalities in the temporal bone. Ideally, both imaging techniques should be used, as different areas can be examined using the two techniques as shown on Figure 4.

Post-operative imaging is important to confirm the correct electrode position and to investigate for any abnormality such as interscalar dislocation or electrode TFO, which can be a potential source of CI malfunction.

I.2.1. Magnetic Resonance Imaging (MRI)

During MRI, the patient is placed into a strong magnetic field. In this field, the magnetic lines of force in the body are aligned with the magnetic field and then return to the ground state when the field is removed. The image is reconstructed based on the time, during which the magnetic lines of force return to their initial state. Because the principle of the procedure, this scan is best used to image proton-rich areas, such as tissues with high water and/or fat content, for example: the brain. On a T2 sequence the channels of the cochlear duct: the scala tympani and the scala vestibuli are well recognized. A pre and postoperative MRI scan can be immensely helpful in assessing whether there is damage on the cochlea and to ensure that the EA is inside the scala tympani and has not caused any damage inside the cochlea.

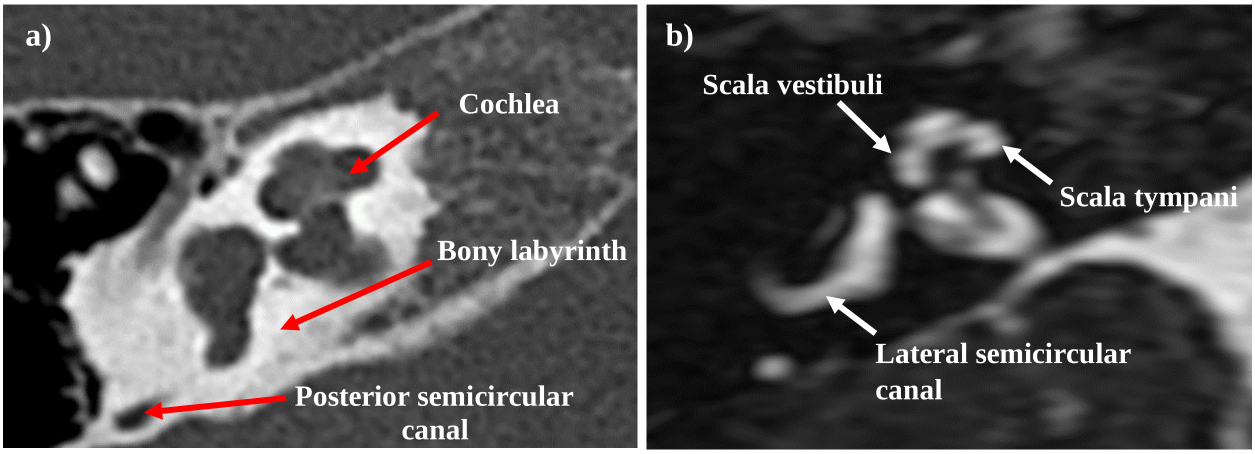

*Figure 4. Comparison of CT and MRI of the temporal bone **a)** CT scan: the air spaces and the bone mass around the inner ear are clearly visible. **b)** MRI: the fluid spaces are more prominent and the two canals of the cochlea, the scala vestibuli and the scala tympani, are also visible.*

The majority of implants on the market are suitable for MRI scan under certain circumstances [25, 26], that are disclosed by the CI‘s company. However, the image may be profoundly distorted by metal artifacts. In case of CI532 at 1.5T scans the speech processor must be removed and must use an MRI kit developed by the Cochlear Company. For 3T scans the magnet must be surgically removed. Usually, the membranous labyrinth can be best viewed on T2 weighted MRI scans in axial and coronal planes, with 0.8 mm thickness.

I.2.2. <u>Computed tomography (CT)</u>

CT, which is an X-ray based imaging technique, shows mainly bones (where most of the rays are absorbed) and air-filled cavities (where there is no absorption, so the area is a well-defined and therefore pure black) with good resolution. A CT scan taken before implantation can be used to determine if the patient is suffering from any anatomical malformation and can establish the necessary electrode type. Postoperative CT can assess the positioning of the EA inside the cochlea to rule out TFO or other defects (tear, partial implantation. Usually in practice, high resolution CT scan is made in the axial and coronal sections, with 0.4 to 0.6 mm thickness.

I.2.3. <u>Fluoroscopy (FL)</u>

Fluoroscopy is another X-ray imaging technique that allows visualisation of moving internal organs (for example the heart) by taking a continuous X-ray image on a monitor. Fluoroscopy is used in a wide range of diagnostic and therapeutic tests and procedures, such as radiological examinations (to visualise the gastrointestinal tract), catheter insertion and manipulation (to guide the catheter through the blood vessels). In CI surgery, the surgical team can follow on real time the insertion of the EA, and can check the result of the surgery, such the final location of the EA.

I.2.4. <u>Human error factor in digital image processing</u>

Nowadays modern computing techniques have spread almost all over the world, and have a massive base in medical science. With the development of technology, we are able to organize surgery in virtual reality, or create robots [27, 28], that can perform some parts of the operation. One of its main advantages is that, with these techniques we can decrease risk of invasive medicine. But these softwares, robots etc. were developed by humans, so their precision is largely dependent on the human error factor. For this reason, it is very important to know how precisely these contributors are able to work.

In most cases, the recordings that are created of the patient, require further processing. These can be manual or automatic measurement tasks. Measurements (length, angle, area etc.) and segmentations (labelled parts of the image) can greatly facilitate the planning of surgery and the success of the intervention itself.

Determination of the cochlear duct's length and/or the length of the electrode array's inserted section, as well as the shape of the cochlea, typical measurements before CI surgery. In order to examine the cochlea in 3D view, we need to segment it from the CT or MRI scan. In this process the specific areas are highlighted with different colour on each image slice. Segmentation can be performed manually, but there are also a number of automatic, semi-automatic methods for it. Packing the created segments together can be reconstructed into a 3D model, so that the parts considered important can be examined in a 3D environment.

In medical image processing the human factor is not negligible [29, 30]. It is important that these tasks are carried out by a specialist or someone who is thoroughly familiar with the anatomy of the examined area. If we intend to use the images for surgical planning, it is crucial that the necessary measurements be correct.

I.2.5. 3D Slicer

3D Slicer is a free, open source image processing and visualisation software [31]. During our research we used this software to carry out segmentation, 3D modelling and measurement tasks. There are a lot of built-in functions and modules, such as: manual or semi-automatic segmentation, registration modules and a wide range of measurement tools. Since the program is open source, anyone can write their own program module, to solve specific tasks, that are not implemented in the 3D Slicer [32]. The modules can also be written in C++ or python programming language.

The software can handle a wide range of image format, including DICOM. The DICOM file is a complex data structure that contains in addition to the image slices: patient data, the parameters of the image, the name of the professional, who took the image, institution, device parameters, date and time etc. A key feature of DICOM is that it groups information into a data set. That is, a patient's CT scan is placed in a file with its identifier, so that the scan cannot be accidentally mixed up with other patient’s data. For our research, the personal information doesn’t required, that the DICOM file contains. 3D Slicer after loading the DICOM file converts it into a .nrrd file, that does not contain any personal information about the patient, only the image slices and their parameters (name, number of pixels and slices). 3D Slicer is able to create virtual 3D models from the segmentation data and these data can be converted into .stl or .obj files, which are the most widely used formats for 3D printers.

I.2.5.1 3D printing

3D printing is a technology that is widespread in the medical sciences. The segmentation results can be printed in 3D and the surgeries are much easier to plan because they are proportionate, nearly anatomically precise due to the wide range of materials (metal, wide range of plastic), and can be produced quickly and cheaply in large quantities [33]. In our case, we can print the cochlea, that was segmented from the individual's CT or MRI scan, and the surgeon or the medical students can practice CI insertion on this model. A further advantage is that the material of a 3D printed model is cheap and it can be printed in several copies, which allows for the substitution of cadaver models in several instances. Our clinic is in close cooperation with the 3D (Printing) Center of the University of Szeged [34].

II. OBJECTIVES

1. To investigate the extent of human error in the manual processing of medical images, in order to decide whether the measurement work can be carried out by students.
2. To develop and implement a measurement algorithm to calculate the correct alignment of the electrode array, especially for Cochlear™ Ltd.'s Slim Modiolar (SM) electrode array.
3. To validate the developed method on a large number of patients and evaluate the results statically.
4. To create digital 3D models of the cochlea and surrounding structures (bony structure, auditory bones, semicircular canals). To plan CI implantation for a cochlea malformation patient and monitoring the insertion of the EA during surgery using fluoroscopy.

III. MATERIALS AND METHODS

III.1. The measurement procedure

At the first stage of our research, we asked 10 students from University of Szeged. 3D Slicer (Win10, v4.11) was used to mark several anatomical landmarks and point-like structures (Table 1., Figure 5-6.) on CT scans. From the measured and reference points, we calculated nine anatomy planes (Table 2.). This data was used to measure the precision of the students by comparing it with reference measurements. Based on the results obtained, we wanted to know whether a large number of measurement tasks could be assigned to students in later part of the research.

Table 1. The anatomical landmarks and point-like structures, that the students had to mark on the CT scans.

Anatomical landmarks	**Point-like structures**
Coronal semicircular canal left and right	Inion
Axial semicircular canal left and right	Nasal peak
Sagittal semicircular canal left and right	Back pole of rostrum
	Mastoid process left and right

Table 2. The anatomical planes that were calculated from the measurements. Abbreviation: L - Left, R - Right, cent - centroid.

Calculated anatomical planes
Plane of axial semicircular canal, both sides (ax_L, ax_R)
Plane of sagittal semicircular canal, both sides (sag_L, sag_R)
Plane of coronal semicircular canal, both sides (cor_L, cor_R)
Mastoid process - Nasal peak – Back pole of rostrum, both sides (m.n.r_L, m.n.r_R)
Nasal peak - Back pole of rostrum – Inion (cent)

The measurements have been carried out on skull CTs of patients of different age groups (1, 4 and 27 years old). The students received the CTs in an anonymized, bar-coded way. To have enough measurement data from one student, these landmarks were determined on three different days, and five times on each day, thus we received 15 measurements from each. Before the test, the students received a basic training (3 hours long) about the usage of 3D Slicer, and recognition of the anatomy points and landmarks on CT records. After each measurement day, the students had the opportunity to ask whether they had marked the points correctly.

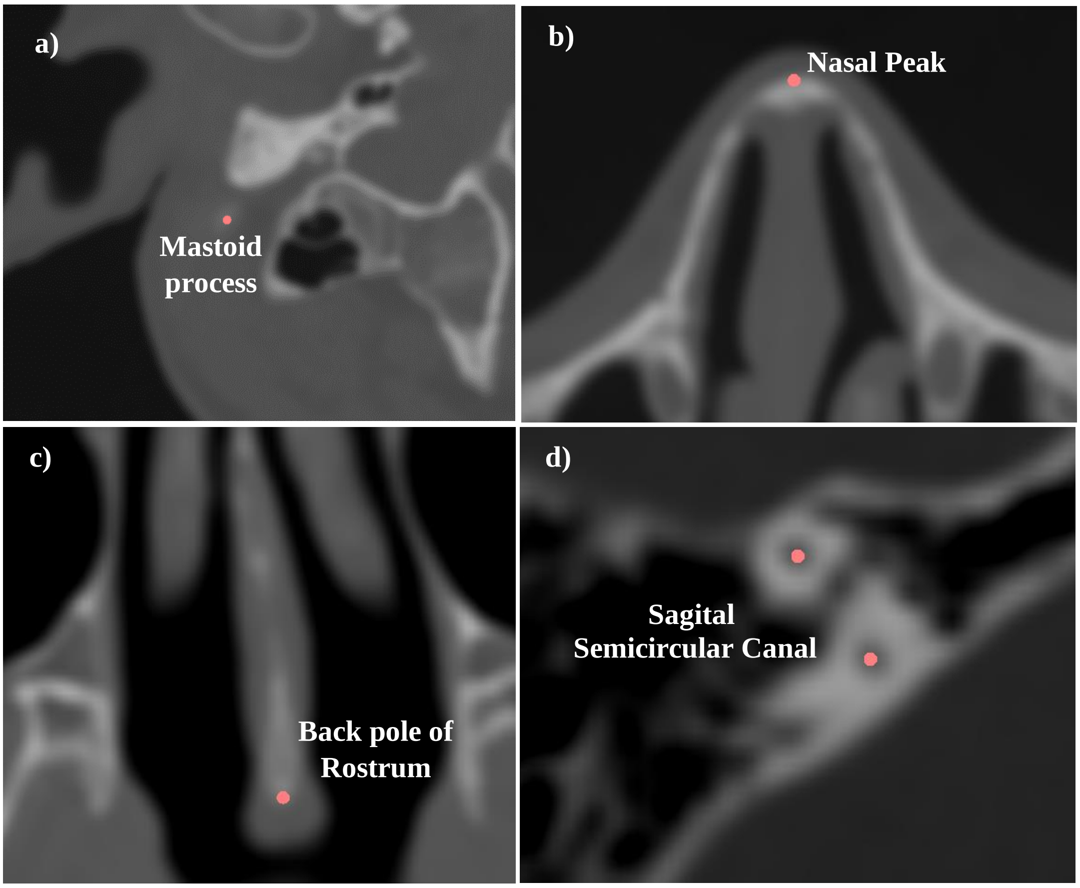

*Figure 5. Examples of the anatomy landmarks that had to be marked. These points were marked on an axial CT scan at the right side. **a)** mastoid process , **b)** nasal peak, **c)** back pole of rostrum, **d)** two points inside the sagittal semicircular canal of the labyrinth*

To determine the semicircular canals, the students had to mark points anywhere within the canal (Figure 5.d). To measure the accuracy, we calculated the planes of the vestibular system from these points. Since a plane can be determined from 3 points, the volunteers had the create 3 measurement points inside the canals. The inion was the most problematic measurement point, because it clearly visible on 3D view only. For this reason, the students had to create a 3D model of the skull from the CT record, and mark the point on the created digital 3D model (Figure 6.). To create this model, they had the segmented a section of the skull, that contains the inion. Since 3D reconstruction image segmentation is important, this allowed us to test the accuracy of both the model creation and the 3D point selection.

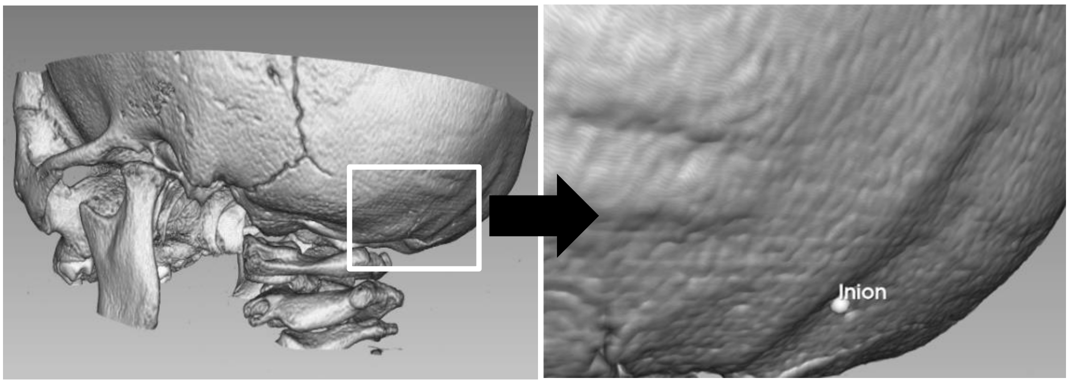

Figure 6. Digital 3D reconstruction of the skull and a magnified section with the marked Inion.

In our study [ref. I.], we observed how the accuracy of the measurements varied between measurement occasions, and we also observed the effect of age. The anatomical planes and angles defined by the points were calculated and compared with the reference dataset. In order to measure student outcomes, we created a reference dataset, prepared by 5 different experienced professionals. Their results were averaged to create the reference measurement dataset. To make faster processing of the measurements, we wrote a Matlab script, to automatically calculate the planes, distances and angles from the 10 students' results. For the statistical processing Excel was used.

III.2. Method to measure the correct alignment of the electrode

Half-banded electrodes, such as the CI532 Slim Modiolar from Cochlear^{TM} Ltd., must be inserted in a special direction (corresponding their curvature). If the electrode insertion happened at the wrong direction, the EA can rewind and TFO occurs [35, 36]. To prevent this, we have developed a semi-automatic algorithm to perform the measurements related to visible surgical landmarks that estimates the correct electrode alignment [ref. II.].

For algorithm development, we used a preoperative CT scan (slice thickness 0.6 mm, no gap, bone kernel) of one of our cochlear implanted patient. Selection criteria were: good quality CT scan (high resolution thin slices up to 0.625 mm, no motion artefact) of the temporal bones, without a reported anatomical malformation and uncomplicated cochlear implantation with a perimodiolar (Cochlear™ Ltd. Slim Modiolar) electrode array. For the measurements we used the before presented 3D Slicer software.

III.2.1. The manual measurement step-by-step

1. On the axial slice, the user marked the incus short process (ISP). The ISP was chosen as a clear anatomical landmark, due to the fact that it is a clearly visible point-like landmark during routine cochlear implant surgery via posterior tympanotomy.
2. The user created the cochlear view [37], with rotation of the coronal slice.
3. Draw two perpendicular lines starting from the round window (RW): first represent the insertion guide of the EA (IG), the second is the orientation marker (OM). The length of the IG line is similar to the real device's parameter (~6.5 mm). The OM line's length was not essential for the measurement. 3D Slicer has a built-in angle measurement tool, to create perfect perpendicular lines.

Thus, three parameters were observed: 1 point (ISP) and 2 lines (IG and OM), as shown on Figure 7.:

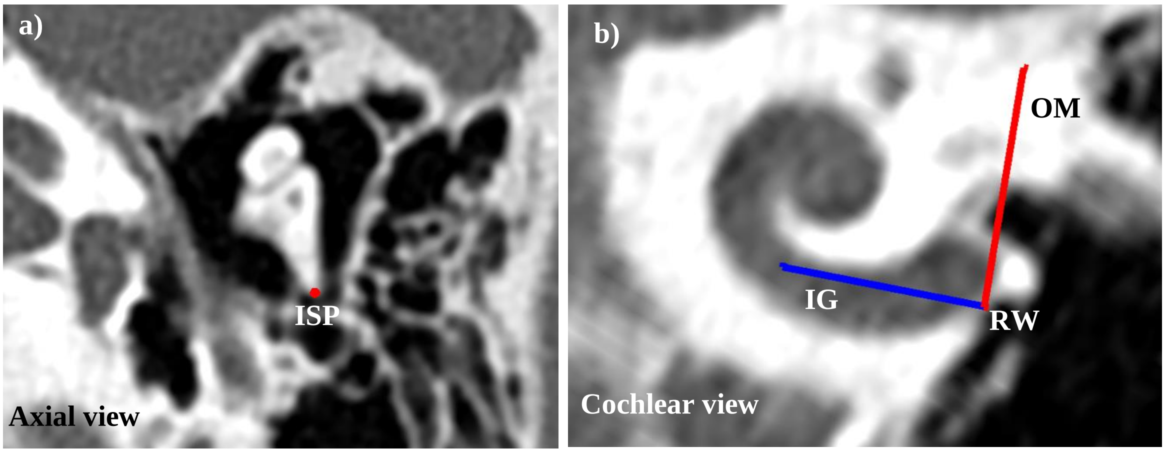

Figure 5. Illustration of the parameters, that required to calculate the correct implantation angle. ***a)*** *The incus short process (ISP) on the left side axial CT scan.* ***b)*** *The lines, that represent the parts of the cochlear implantation tool. Red line as the orientation marker (OM), blue line as the insertion guide (IG). These lines were drawn on the left side in cochlear view and crossed each other at the round window (RW).*

III.2.2. Scripted module to 3D Slicer

To obtain the correct alignment of insertion from the above three parameters, complex mathematical calculations are required. As mentioned before, 3D Slicer is able to develop custom modules, that are not built in or not downloadable. The software minimum requirements are not so high, it can be run on an average PC (4GB RAM, Display resolution of 1024×768, GPU 2GB memory). Therefore, this calculation module is useable for most of the users. Since we needed calculations that are not in the program, for this reason we had to implement a separate module for the 3D Slicer (Figure 8.). Firstly, the module calculates the plane defined by the lines IG and OM. This is the cochlear view itself, which is the ideal plane for the EA insertion. Then this plane was rotated 90 degrees along the line of OM to obtain the plane perpendicular to the cochlear view. Although the surgeon is able to visualize the depth (3D view) with the surgical microscope, estimation of angles and planning the surgery is easier and more accurate in one plane (2D view). For this reason, the program projected the ISP into the previously mentioned plane (cochlear view rotated by 90 degrees). Finally, the angle between OM and a virtual line, that connect the ISP with the RW, is defined.

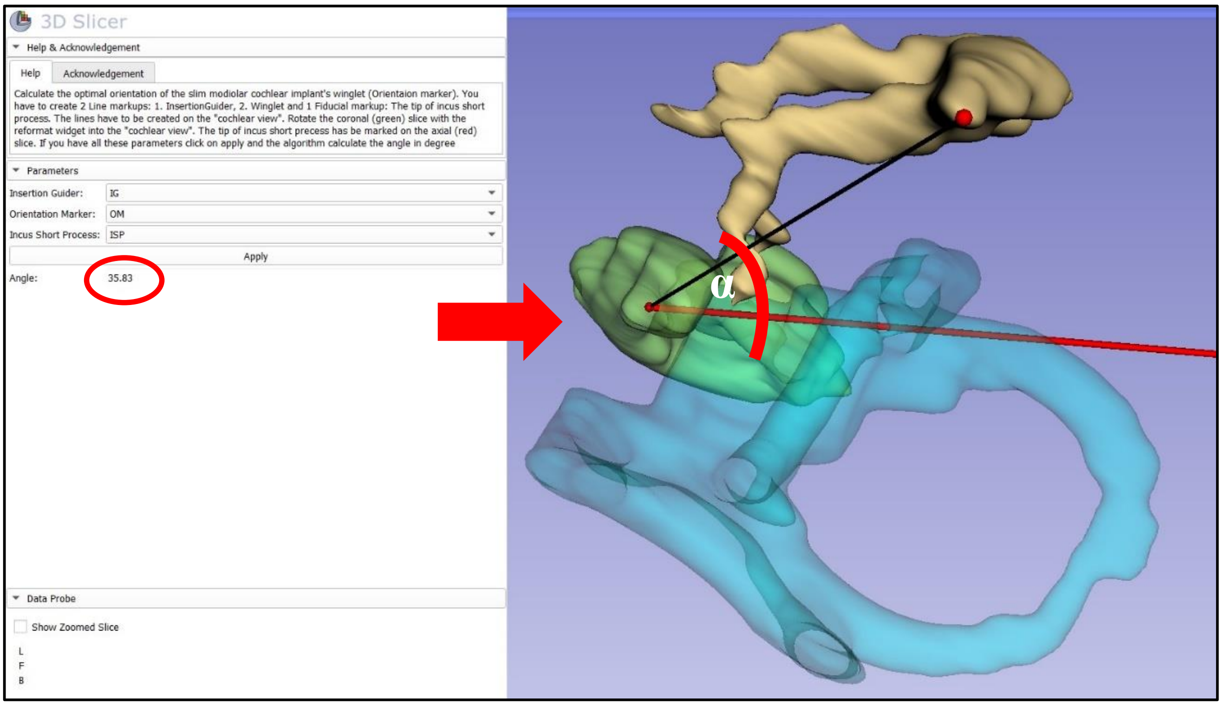

Figure 6. Our self-made implantation angle calculation module and a 3D illustration of the calculated angle with the used anatomical landmarks. On the left side of the picture shows the control panel of the module: after giving the 3 parameters (Insertion Guider, Orientation Marker and Incus short process), clicking on the Apply button the program will calculate the angle in degrees, which is marked with an alpha in the 3D model. The view of the 3D model is closely equal to the view of the implantation procedure.

III.3. Validation and processing of the data

After applying the algorithm on one patient's imaging data, we have collected the last 3 years of all our implanted patients who had preoperative CT scan [ref. III.]. From these, we selected those that met our requirements: high resolution temporal bone CT, malformation-free and implanted with SM array. In total of 80 CT scans were used. In the first few cases the results by the module were checked by manually counting and the angles were validated on digital 3D models using 3D Slicer's built-in angle measurement tool. The results obtained were subjected to statistical tests using R-Studio (R version 3.6.3, Windows 10).

III.4. Real time insertion recording

Since the measurement method was developed for non-malformation cases, a different method was chosen for our next presented patient [ref. IV.]. The patient is a 1-year-old boy with bilateral hearing loss, whose CT and MRI scans revealed type III. cochlear hypoplasia [38] of both cochlea (Figure 9.). Patients with this lesion have a normal basal turn of the cochlea, that is followed by a vestigial second turn, making only half a turn, and the third turn is absent. The internal structure (scala tympani, media and vestibuli) is not damaged. This cochlear abnormality may be associated with a malformation of the organ of balance, in our case, a partial absence of the lateral semicircular canals.

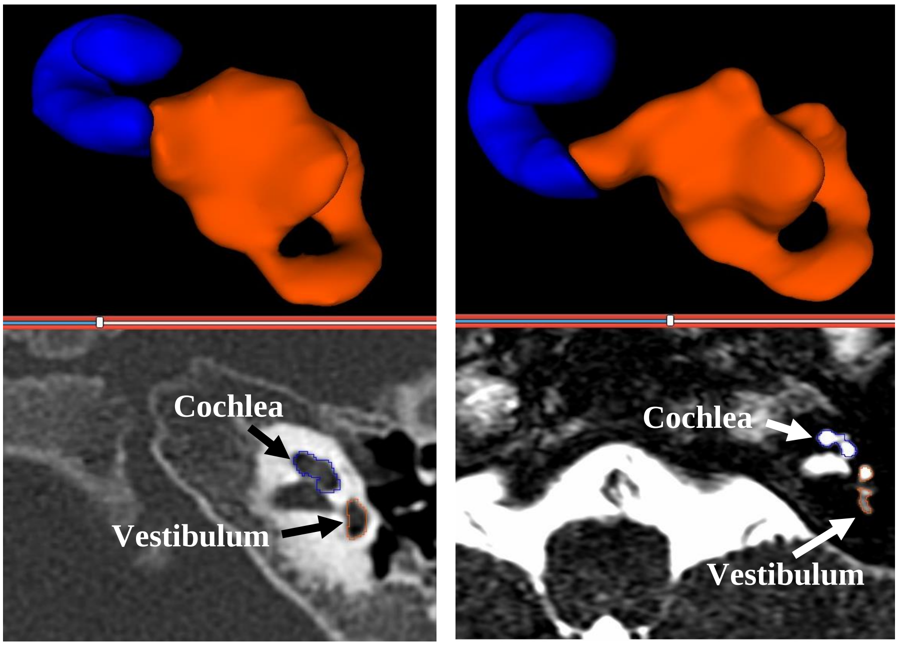

Figure 7. 3D models form the preoperative CT scan (LEFT) and from the MRI scan (RIGHT). On both images seen well the abnormality of the semicircular canals, and the vestigial second turn of the cochlea. On the MRI scan we could establish, that the inner structure of the cochlea is not deformed, scala tympani and scala vestibuli are present.

The cochlear implantation of both ears was performed at the Szent-Györgyi Albert Clinical Center of University of Szeged, the electrode used was the Cochlear^{TM} Ltd.'s Slim modiolar perimodiolar electrode (CI632). The intraoperative imaging was performed by Siemens Artis Pheno (Siemens Healthcare GmbH, Erlangen, Germany) robotic DSA system.

IV. RESULTS

IV.1. Distance between measured and reference point-like landmarks

We measured the distance between only the point-like objects on both sides: mastoid process, nasal peak, back pole of rostrum and inion. Due to the circular nature of the semicircular canals the plane could be determined based on the points marked. However, the distances between the points could not be measured.

The results are mostly similar of the 1 and 4 years old patients. On the 27 years old patient's scans the students achieved larger inaccuracy, so we concluded that age represents a slight influencing factor in this examination (Figure 10.). The measurements were the most inaccurate at inion. There the average distance between the references was 15 mm, but there were outstanding values: 30-35 mm. The other problematic point was the back pole of rostrum, there we measured approximately 5 mm difference from the reference data. The most accurate results, that were closest to the reference data, were achieved on the mastoid process and nasal peak, there the distance from the reference data was 0.5-1 mm (Figure 10.).

Since it was possible to check their results between the measurement occasions, we examined whether there was a change between the results of the 3 measurement days. A minimal improvement was obtained (average improvement of 0.1-0.2 mm), but the selection on the 3D model did not improve significantly between occasions.

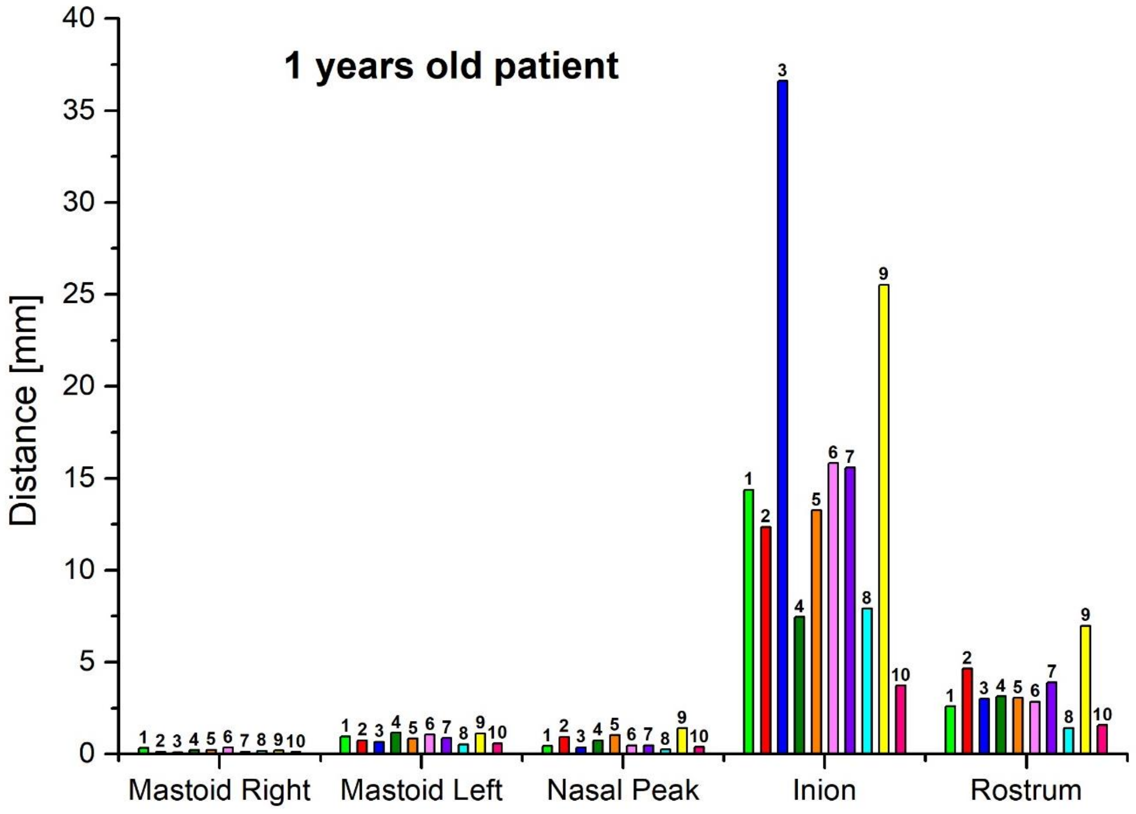
1 years old patient
Distance [mm]
Mastoid Right
Mastoid Left
Nasal Peak
Inion
Rostrum

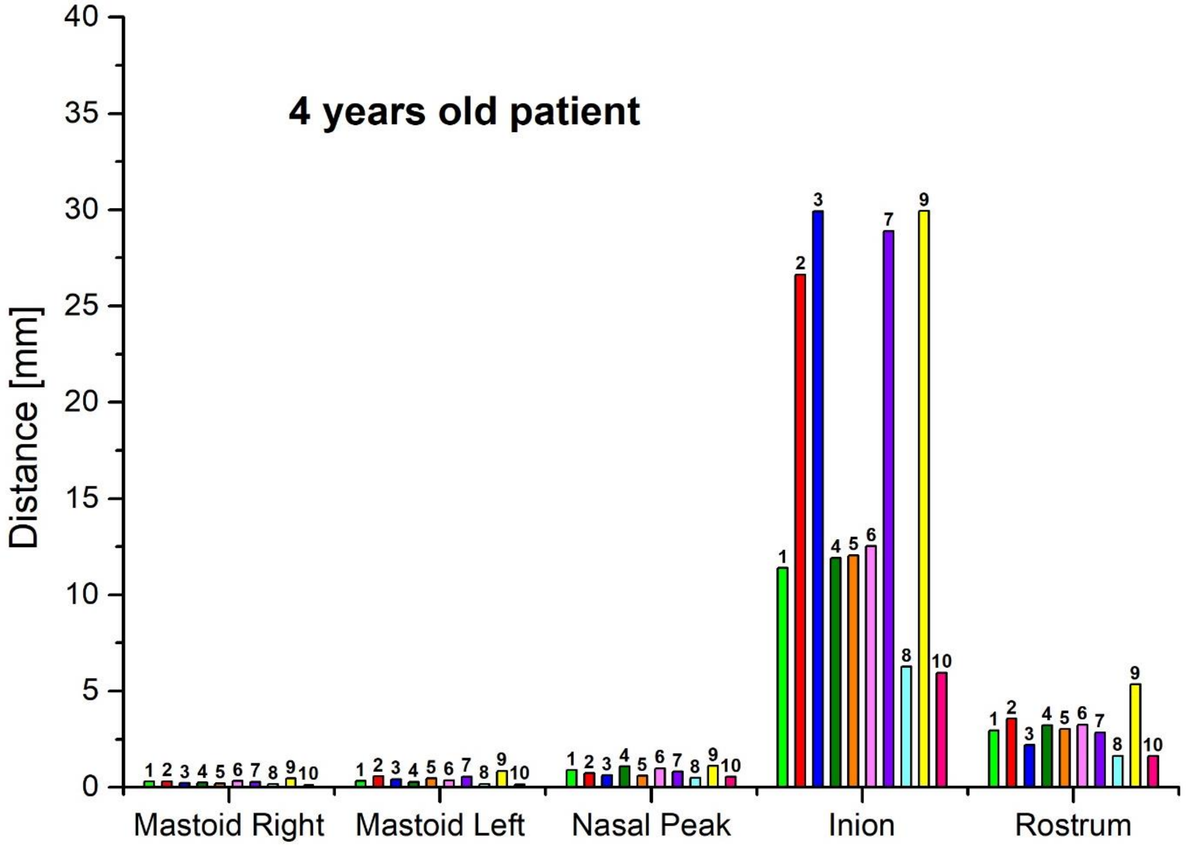
4 years old patient
Distance [mm]
Mastoid Right
Mastoid Left
Nasal Peak
Inion
Rostrum

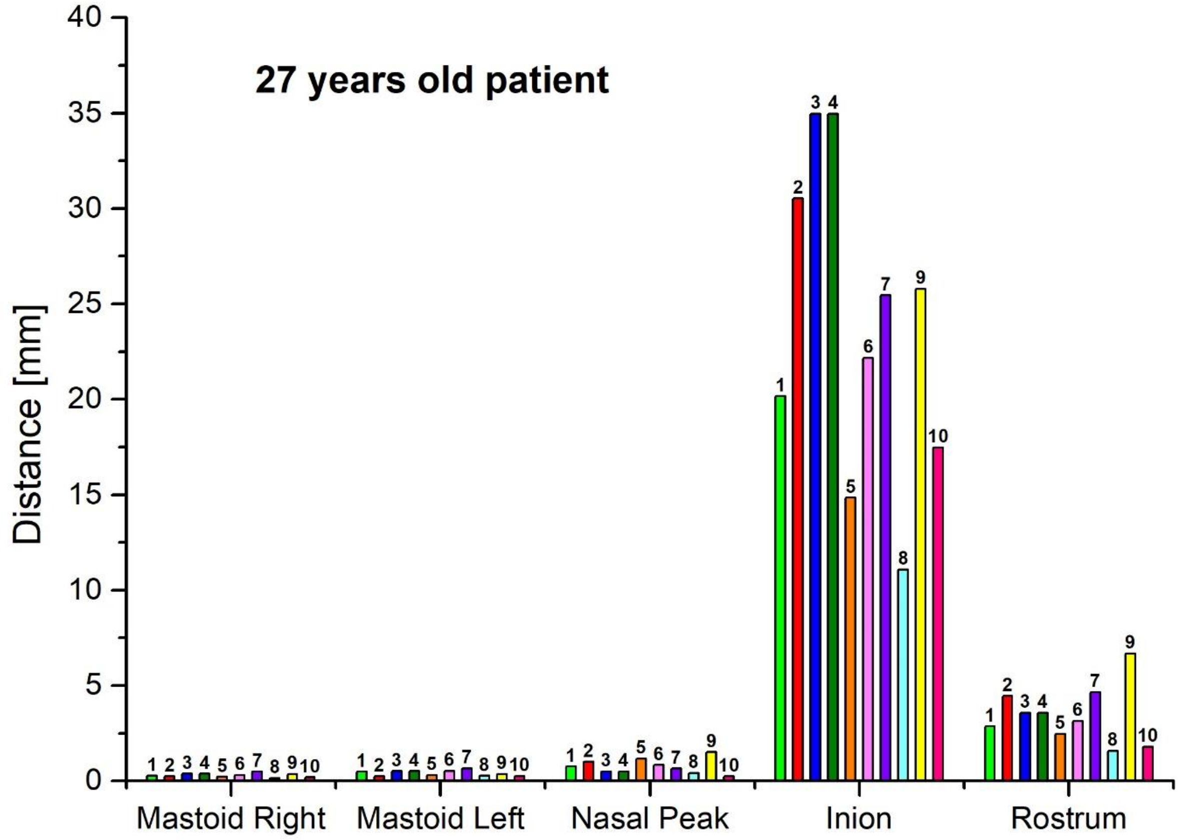

Figure 8. Distances between the measured and reference point-like landmarks of all patients. The graphs show average over 15 measurements for each student. The same numbers above the columns and the colors are assigned to same students. On the graphs see well, that the inion was the most inaccurate point. The best results were got at the mastoid process and the nasal peak.

IV.1.1. Angles enclosed by the calculated and reference planes

We compared the angle between the planes calculated from the students' results and the reference values. Ideally the planes would overlap completely so the result would be approximately 0 degrees. This is closely achieved in the case of the *Mastoid process - Nasal peak - Back pole of Rostrum* lines (the differences are mostly 0.5-1.5°), as the students were able to mark these points with highest confidence.

The students achieved the similar results, but there was a greater variance between their measurements of the semicircular canals (Standard deviation (SD) ~ 4-6°) for all cases (Figure 11.). For the centroid line (*Nasal peak - Back pole of rostrum - Inion*), the difference was large, for 4 to 27 years old patients 10-15° difference was measured. This could be because this line also contains the inion, which was the most inaccurate point during the research.

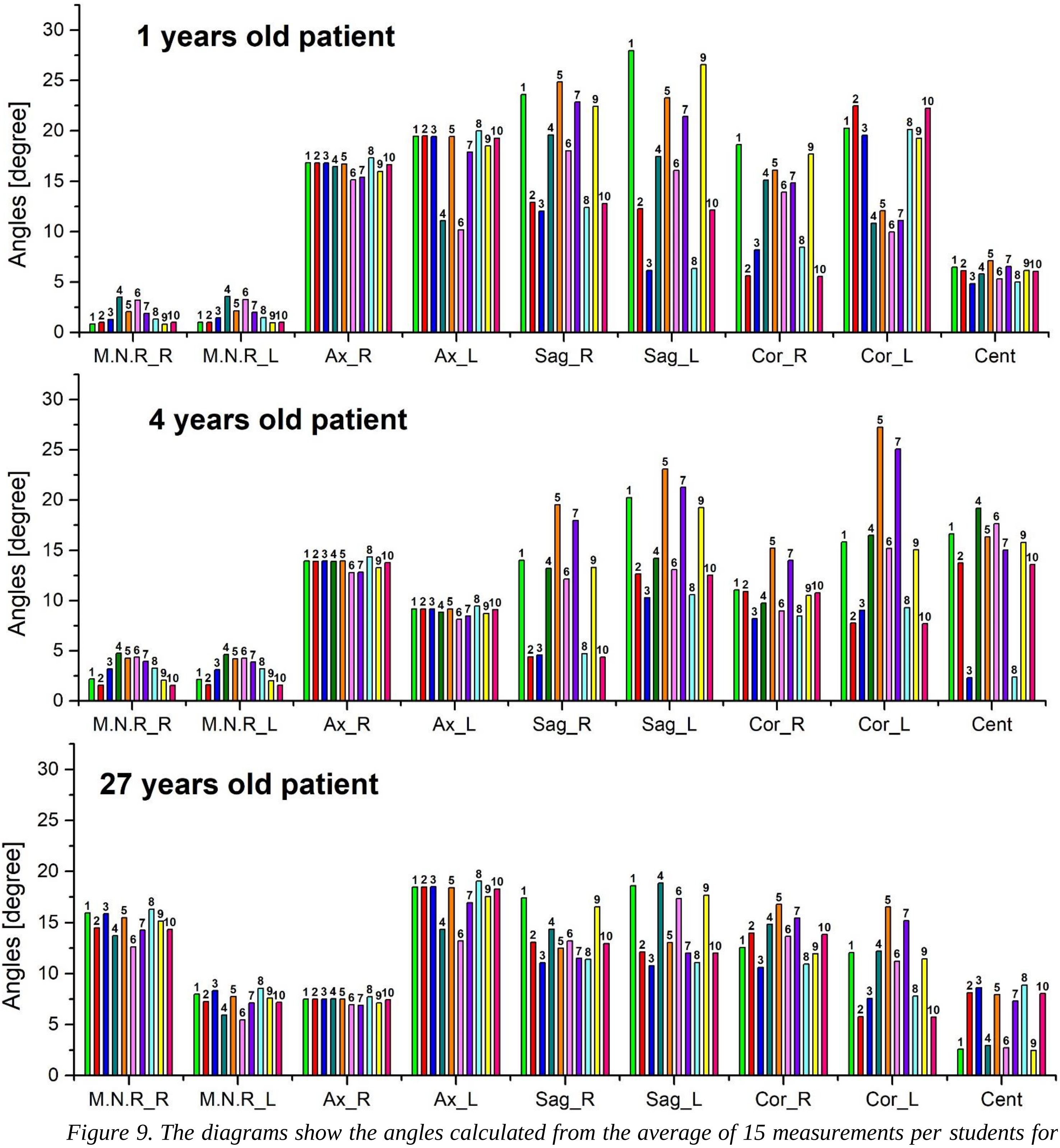

Figure 9. The diagrams show the angles calculated from the average of 15 measurements per students for three patients. This is the angle enclosed by the planes calculated from the measurements of the professionals and the planes calculated from the measurements of the students. Same numbers above the columns and the colors are assigned to same student. The optimal result should be zero degree, but we got approximately 15° differences from the professionals' measurements.

IV.2. Correlations of the correct electrode insertion angle

Using our method outlined in Chapter III.2., we determined the correct implantation angle (mean 45.0-47.2° ± 10.4-12° SD) from the measurement data of 80 different patients using our custom-made python scripted 3D Slicer module. The results obtained by the program were checked by manual counting in the first few cases. The mean age of our cohort was 22.7 years± SD 24.8 years. Age (when the CT scan was taken) and sex distribution are shown in Table 3.

Table 3. Sex and age distribution of patients studied.

	Quantity	Youngest [years]	Oldest [years]	Average [years]	SD [years]
Female	36	1	77	24.1	25.4
Male	44	1	75	21.5	24.5
ALL	80	1	77	22.7	24.8

In this study, the ratio of female to male patients was nearly 1:1. The youngest patient in our study was 12 months old. For the statistical analysis we used the free-to-download R statistical package (R version 3.6.3, IDE: R Studio, platform: Windows 10). The basic statistical results of the measurements are presented in Table 4.

Table 4. Basic statistical results of the measurements.

	Min. Angle	1st Quartile	Median	Mean	3rd QUARTILE	Max. Angle	SD
Left Side	20.5°	34.8°	44.0°	45.0°	53.7°	72.4°	12,0°
Right Side	20.9°	40.3°	45.6°	47.2°	53.0°	75.3°	10.4°

IV.2.1. Correlation with sex

Previous studies have raised the possibility of the differences of the cochlea anatomy between females and males [39]. Before a two-sample t-test, it is necessary to check the equality of the variance. The p-value of the variance test was 0.135 on the left side and 0.084 on the right side (α=0.01). The equality of variance was accepted due to the $p>\alpha$ on both sides. Then a two-sample t-test was performed which included the angle and the sex of the patient (α=0.01). The p-value on the left side was 0.124 and on the right side it was 0.115. The p-values were higher than 0.01, therefore the sex of the patient had no statistically significant effect on the size of the angle.

IV.2.2. Correlation with age

We examined, whether the age of the patient has any effect on the calculated angles. Since age is a discrete variable, a one-way Anova test was used. The p-value on the left side was 0.712 and on the right side it was 0.160. Because the p-values were higher than 0.05, age has no statistically significant effect on the size of the angle.

IV.2.3. Correlation with measured side

Finally, we examined whether there are any linear connections between the measurements on the left and right side. To check this a Pearson's correlation test was used (Figure 12.). This correlation test requires a normal distribution of the data set. To check this requirement, we performed a Shapiro-Wilk test (α=0.05). The p-value was 0.187 on left side, and 0.133 on the right side. Because the p-values were higher than 0.05, it was accepted that the angles follow normal distribution on both sides. The Pearson's correlation coefficient was 0.513.

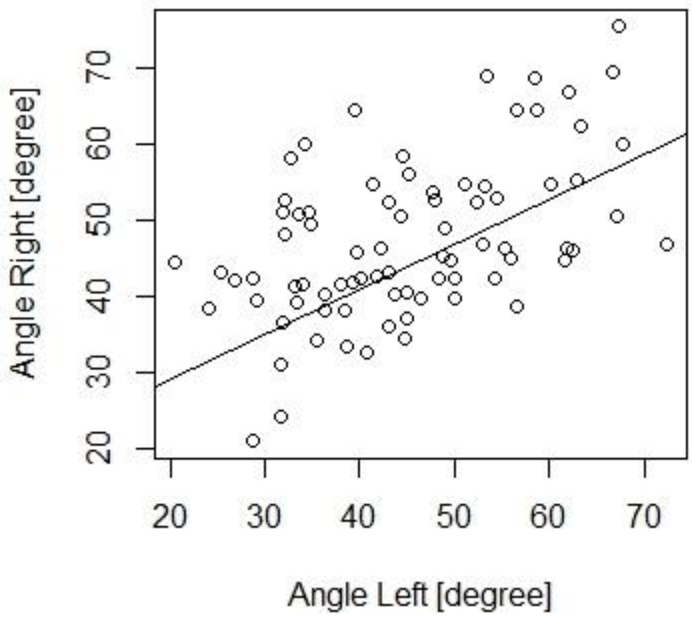

Figure 10. Linear correlation between the side and the size of the angle. As see there is a very weak positive linear correlation, correlation coefficient is 0.513.

A significance test was performed for this correlation coefficient. The Student's t-distribution value was 5.271 and $t_{78, 0.05}$ = 1.99 (df=78, α=0.05, p= 1.172e-06). Because $|t| > t_{78, 0.05}$ and $p<\alpha$ the correlation coefficient is significantly different from zero, so there is a very weak positive linear correlation between the measured side and the size of the angle, as showed in Figure 10.

IV.2.4. <u>Electrode insertion angle in known tip fold-over patients</u>

The insertion angles of the EA were compared in our 80 patients and to five TFO cases that occurred in our clinic. We determined also the insertion angle of these patients using their preoperative CT scan (Table 5.). The insertion angle was then compared to cases where a TFO occurred to the measured average angle. Although angles of Patient 2 and Patient 3 are very close to the mean value, the other three patients' results are close to the endpoint of SD range.

Table 53. Determined angles of the patients where tip-fold over occurred. Marked with bold font at the side of the implantation

	Left Side Angel [°]	Right Side Angle [°]
Patient 1	35.4	**34.2**
Patient 2	**44.9**	37.1
Patient 3	52.9	**46.9**
Patient 4	**54.3**	42.2
Patient 5	**55.9**	44.9

IV.3. Imaging during cochlear implantation surgery

The process of electrode array insertion into the cochlea was monitored by a C-arm DSA device on both sides, using its fluoroscopic function (Figure 13.). After implantation of the second implant, a cone beam CT scan was taken with the same C-arm DSA device. As seen on Figure 13-14. no complications were detected by video fluoroscopy and cone beam CT scan.

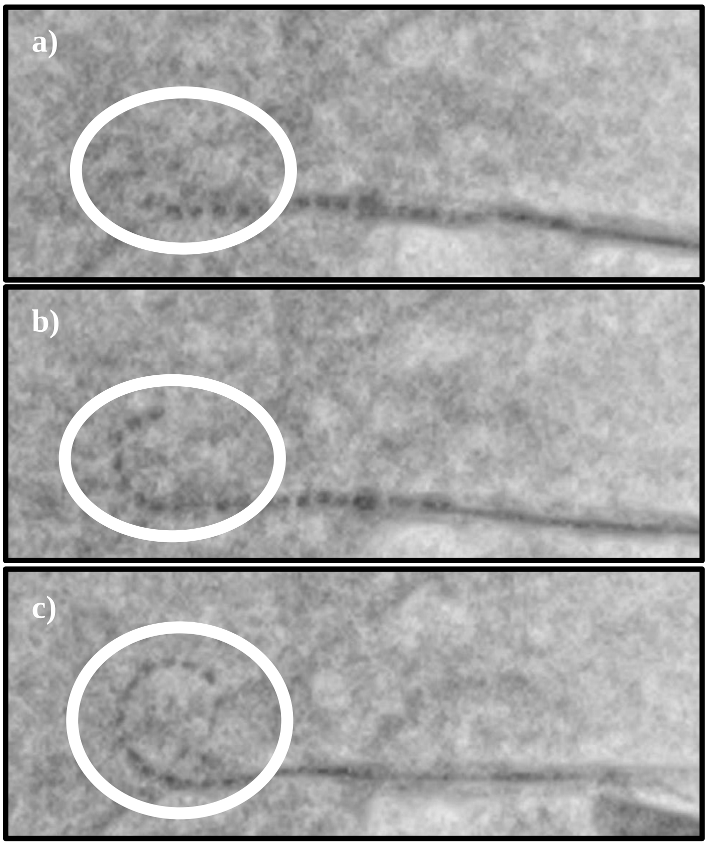

Figure 11. Image captures at three different time from the video of the cochlear implantation process. The video was captured by a C-arm DSA device, using the fluoroscopic function. The insertion of electrode was free of any complications.

During the first programming of the external speech processors for the implant, which was performed four weeks after surgery, the child had a clear auditory experience. The child listened with interest to the electrical signals perceived as sound on both sides of each electrode.

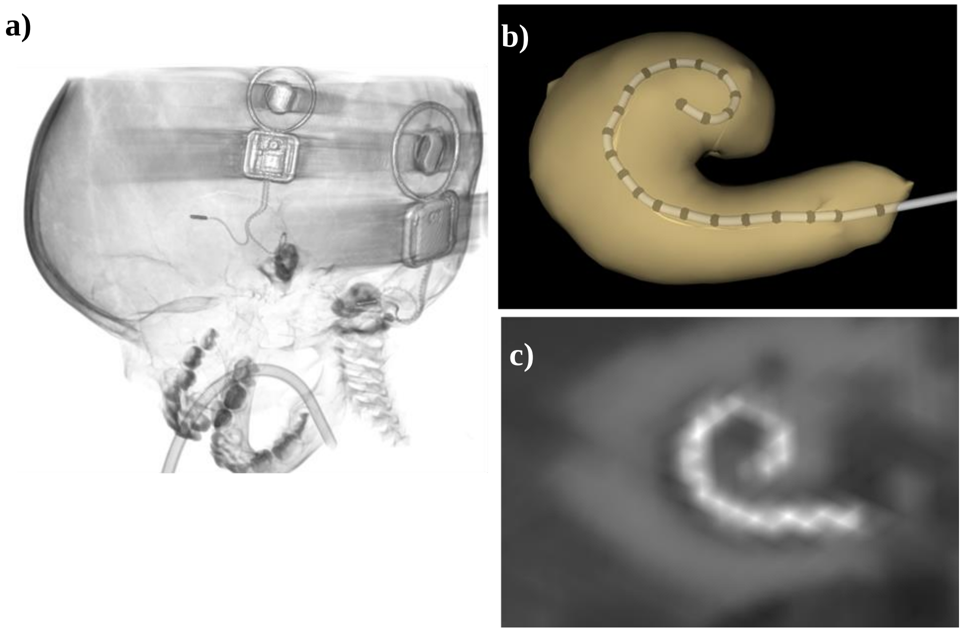

Figure 12. ***a)*** *Volume rendering created from the postoperative cone beam CT scan using 3D Slicer. On this image we can see both CI devices, the inner and outer parts also visible.* ***b)*** *3D reconstruction of the left side cochlea including the inserted electrode array. The cochlea was segmented from the postoperative CT scan. For better visualization we made a sematic tube-like model of the EA, that not represent the electrode's real positions inside the EA,* ***c)*** *Postoperative CT scan of the left side cochlea. The slice was rotated into the cochlear view. The picture shows that the implantation was successful, the EA extending through the canal of the cochlea.*

V. DISCUSSION

V.1. Human error factor

Measurement accuracy is one of the cornerstones of our research, so we observed the accuracy of the anatomical structures' identification on the provided CT scans by medical students. We used anatomical points that may relevant to the field of otolaryngology. To simulate the changing anatomy with increasing age, the students performed measurements on CT scans of 3 patients at different ages. Overall, we found that age was not a determinant factor in the recognition and assignment of the landmarks. We found that there was no significant positive change (0.1-0.2 mm) in the accuracy of the measurements between the 3 measurement sessions. The accuracy may be potentially improved if measurements are taken more than 3 sessions or after a more detailed training.

The investigation found that, volunteers are reliable enough to recognize point-like structures such as the mastoid process and the nasal peak. We noticed small differences (Figure 10.) between the students inside of Inion. One of our future goals is to use 3D printed models to plan and try the surgery, so we tested the students' accuracy to create and process 3D models. Thus, more advanced users can determine better 3D model planning and final outcomes. The largest deviations were found in the case of semicircular canals (Figure 11.). This can be explained by the fact that very small volumes had to be marked and, in such dimensions, an error of up to 1 mm can cause large deviations. These results suggest that assessment and identifying anatomical structures using 3D Slicer software should only be given to students and young professionals under guidance of an experienced professional.

V.2. Definition of the correct insertion angle

The next stage of the research was to investigate the average correct orientation of the CI electrode array's OM, relative to anatomical landmarks. For this, we developed a new, custom python scripted module into 3D Slicer, and we performed the measurements on 80 cochlear implanted patients' preoperative CT scans. We carried out statistical analysis on the results, and this indicated that the correct alignment of the OM in a successful CI insertion is approximately 45.0°-47.2°±SD. We investigated also the impact of the age and the sex of the patients on the correct insertion angle, and the statistical results did not show any connection between them.

However, there was a weak positive linear correlation observed between the measurements on the left and right sides.

The angles were calculated with the electrode array inside the insertion tool. In this position the insertion tool prevents the electrode array from moving away. Once the electrode is inserted into the cochlear duct and the insertion tool is removed, the electrode reaches more "comfortable" position, which is not equivalent to the position it takes with the insertion guider. Therefore, we did not perform the measurements on the postoperative scans, because the resulting angle would not be representative.

V.2.1. Calculation of the insertion angle

We used 3D Slicer during our research to perform medical image processing. This program is open-source, that is and advantage and disadvantage also. The positive side, that we are able to develop new modules, that the research required or modify the software core code. These self developed modules can be download by anyone, and due the large number of them, it is hard to find one that's useful for the actual work. These downloadable packages are not validated for medical applications, so they have to be done by experts, in contrast to medical applications, where the result data is guaranteed to correspond to reality (for example when a length measured by a user is 2.5mm it can be accepted without validation).

3D Slicer software is able to mark anything on the loaded images with their 3D coordinates. We are able to rotate slice into non-conventional plane (different from, axial, coronal and sagittal). With this feature we could rotated the coronal plane to the cochlear view, and marked and measured the IG and the OM. These 3D points and vectors were loaded into our custom python scripted 3D Slicer module, which was used to calculate the angle. The limitation of this technique is the manual measurements on the CT scans. If the user cannot mark the landmarks or create the exact cochlear view, the angles may be distorted.

Our study measures the correct orientation of the SM electrode's OM, but the method can be adopted to other half-band electrodes e.g., the Cochlear™ Ltd. Nucleus® Slim Straight and Contour Advance. In case of half-banded electrodes, the position of the OM related to the position of the modiolus is to be considered and the calculated angle is to be corrected accordingly (e.g. 180° should be added if the marker or guide wire is to be positioned caudally). For the other type, the so-called full-band electrodes do not require such measurements, because this electrode design allows their insertion in any orientation angle (e.g. Med-El®: FORM® Series, CLASSIC® Series). Based on our experience, other contributing factors are likely to include: i) too fast or forced insertion of the very delicate electrode array [40], ii) incomplete loading of the array with the tip remaining and curving already outside the IG, iii) incorrect loading of the electrode array which causes the array to stuck in the slot of the IG, iv) incorrect insertion trajectory vector for example if the array is directed too much towards the medial or lateral wall of the cochlea which also may cause bending of the IG. In this situation the deformed IG's slot may expand which results in electrode array insertional failure. It is assumed that incorrect insertion trajectory can also be caused by a narrow or insufficiently extended RW or the presence of a pronounced fissula ante-fenestram.

V.2.2. Insertion angle in tip fold-over cases

Until recently, TFO of the electrode array was only of a small probability (~0,80%) seen in lateral wall electrodes [35]. However, with the new generation of the CI, thin perimodiolar EA model, TFO can occur in ~4.7% of cochlear implanted cases.

In this study we calculated that the average angle of the orientation marker to the ISP in successful implantations is approximately 45.0°-47.2°±SD which was verified with a confidence interval of 98%. We determined also the insertion angle on five known TFO case's preoperative CT scan, and we have found, that only some of the angles fell outside the average range, which suggest that the TFO was caused by other factors (too fast insertion, improperly loaded electrode, forced insertion) not the orientation of the marker, for which our method was designed. Although the values suggested that the further the diversion from 45.0°-47.2°±SD, the increased chance of TFO.

V.2.3. Potential impact of the study

Anatomical landmark guidance is becoming important for the future of CI surgery [41] due to technological advancements and improvements in surgical techniques. In our research we used the CT data of patients, who were implanted with SM electrode array. The user guide [42] of this device lacks a precise numerical recommendation on where the orientation marker should point during the insertion of the electrode array, which may lead to potential misalignment. Our study intended to quantify the optimal position of the orientation marker relative to the visible intraoperative anatomical landmarks. Furthermore, a numerical approach is likely to aid in personalising the electrode array insertion, since the basal turn of the cochlea may vary between individuals [43]. This may also reduce the chance to take any damage on the basilar membrane by inserting the electrode array, which could result in decreased residual hearing preservation [44]. The use of landmark based and numerical approach is also very valuable for training less experienced surgeons to standardise the process leading to improved consistency through an evidence based approach [45].

V.3. Monitoring the electrode insertion

The requirement for cochlear implantation is to take the implantation process with an EA that allows for better speech understanding, while minimising insertion trauma [46, 47]. A thin PM electrode array combines these advantages, but as discussed earlier, TFO can occur inside the cochlear duct during insertion [45, 48, 49]. If this complication is detected before wound closure, there is a good chance that it can be corrected intraoperatively. Our method presented here, real-time tracking of the EA within the cochlear duct is possible. The membranous labyrinth, that contains the functional system of the cochlea is surrounded by compact bone, for which the array cannot be visualized inside the cochlea with the operating microscope, and therefore the abnormal position of the EA is not detected by the operating surgeon. Real-time imaging, enables immediately detection of the electrode array, if it leaves the vicinity of the modiolus, turns back, breaks or enters into the balance organ. Depending on the type of electrode array, by slightly retracting or removing it completely, it has a good chance of being corrected and repositioned.

In our case with type III cochlear hypoplasia, the basal turn was of average size and shape. In cochlear hypoplasia malformation, implantation of a short straight electrode array is recommended [18]. Nevertheless, we chose a thin, pre-curved electrode because we considered it important for the speech development of our 1-year-old patient to position the electrode array closer to the modiolus and to minimize trauma to the cochlear structure.

In our case, no abnormality was observed using the fluoroscopy method. We confirmed that the electrode array was fully insertable and close to the modiolus based on 3D digital models and low-dose-rate volume tomography [50], which are performed after electrode insertion.

VI. CONCLUSIONS

VI.1. Examination of human error factor

In this study, we measured the accuracy of young medical students when they had to select different anatomical structures on CT scans. We used anatomical points that may help otorhinolaryngology researches. The one goal of this test was to give a useful guideline for the supervisors to establish how may be their students' accuracy in manual image processing measurements. To simulate the changing anatomy with increasing age, the students performed measurements on CT scans of 3 patients of different ages. Overall, we found that age was not a determinant in the recognition and assignment of the landmarks. We found that there was no significant change in the accuracy of the measurements between the 3 measurement sessions. This can probably be improved if measurements are taken more than 3 sessions.

The investigation concluded that, volunteers can reliably recognize point-like structures such the mastoid process and the back pole of the rostrum. We noticed small differences between the students inside of Inion, but the 3D model processing caused big inaccuracy. The largest deviations were found in the case of semicircular canals, which can be explained by the fact that very small volumes had to be marked and in such dimensions an error of up to 1 mm can cause large deviations and that one or two students did not select the canals correctly. The results showed that this type of work should only be given over to students and young professionals under the supervision of an experienced professional. With our research, we hope to have been able to help research groups who do image processing work with students.

VI.2. Finding the optimal insertion orientation of CI electrode array

Due to the differences in the individual anatomy, this ~45.0°-47.2°±SD, angle range is not suitable for all cases. Although there is a weak positive correlation between the angles of the left and the right side, it is necessary to take measurements bilaterally if both sides are to be implanted.

Our results can serve as valuable additional information for the surgeon in planning and performing the implantation procedure. During electrode array insertion, the plane of the basal turn of the cochlea is not visible. The 3D models and the calculated angles provide deeper knowledge of the individual anatomy pre-operatively. Before the insertion of the electrode array into the RW, the surgeon can align the OM towards the ISP using the patients' preoperative calculated angle. This angle considers the individual anatomy of the patient and guides the surgeon based on visible anatomical landmarks. Thus, using the quantified angle, the surgeon does not have to rely exclusively on intuition of the cochlear basal turn during orientation. Furthermore, consideration of cochlear anatomy during electrode array orientation potentially reduces complications such as TFO and interscalar dislocation.

VI.3. CI implantation in a hybrid operating room

The aseptic environment of the hybrid operating room combines surgical equipment, instruments, operating tables, operating lights, equipment management systems, together with advanced imaging systems and offers the possibility to perform combined imaging-guided procedures with minimally invasive methods. These full modern operating rooms also allow a combination of imaging-guided surgery and open exploration also. On the other hand, if there is a need to convert a minimally invasive surgery into an open exploration procedure, these spaces allow for a seamless transition by providing all the necessary technical implementation and staffing in one location. In addition, this technology has led to the development of new procedures that offer greater options for patients with complex disease [51-53].

We recommend the introduction of intraoperative imaging for cochlear implantation centres to ensure well-controlled, minimally invasive procedures. We expect new innovations from the developers of C-arm X-ray fluoroscopy equipment in the routine, easy use of the devices, even in the specific field of head and neck surgery. Intraoperative imaging replaces routine radiographic examination in multiple views on the first postoperative day, which may be of limited value in age-related non-cooperation due to motion artefacts and may require repeated imaging.

By using these C-arms CT devices in a protocol-based manner, correction can be performed in one sitting due to an abnormally positioned electrode array, consequently voiding the need for a post-operative radiographic examination and avoiding revision with additional anaesthesia and surgical stress.

VII. References

1. Batthyany, C., A.R. Schut, M. van der Schroeff, and J. Vroegop, *Translation and validation of the speech, spatial, and qualities of hearing scale (SSQ) and the hearing environments and reflection on quality of life (HEAR-QL) questionnaire for children and adolescents in Dutch.* Int J Audiol, 2022: p. 1-9.

2. Hyams, A.V., M. Hay-McCutcheon, and F. Scogin, *Hearing and quality of life in older adults.* J Clin Psychol, 2018. **74**(10): p. 1874-1883.

3. Sperati, G., *[Alessandro Volta and first attempts at electrotherapy of deafness].* Acta Otorhinolaryngol Ital, 1999. **19**(4): p. 239-43.

4. Moore, J.A. and H.F. Teagle, *An Introduction to Cochlear Implant Technology, Activation, and Programming.* Lang Speech Hear Serv Sch, 2002. **33**(3): p. 153-161.

5. Seitz, P.R., *French origins of the cochlear implant.* Cochlear Implants Int, 2002. **3**(2): p. 77-86.

6. Lenarz, T., *Cochlear implant - state of the art.* GMS Curr Top Otorhinolaryngol Head Neck Surg, 2017. **16**: p. Doc04.

7. Jansen, C., *Posterior tympanotomy: experiences and surgical details.* (0030-6665 (Print)).

8. Luers, J.A.-O., K.B. Hüttenbrink, and D. Beutner, *Surgical anatomy of the round window-Implications for cochlear implantation.* (1749-4486 (Electronic)).

9. Klabbers, T.M., F. Heutink, W.J. Huinck, W.J. van der Woude, B.M. Verbist, and E.A.M. Mylanus, *Intracochlear electrode array position and cochlear implant outcomes using the nucleus slim modiolar electrode and the extended round window approach: a follow-up study.* Eur Arch Otorhinolaryngol, 2022. **279**(10): p. 4735-4743.

10. Aidona, S., P. Stagiopoulos, G. Kyriafinis, and J. Constantinidis, *Self-Determination Calibration for Cochlear Implant Rehabilitation*. 2019. p. 121-154.

11. Spiegel, J.L., D. Polterauer, J.M. Hempel, M. Canis, J.E. Spiro, and J. Muller, *Variation of the cochlear anatomy and cochlea duct length: analysis with a new tablet-based software.* Eur Arch Otorhinolaryngol, 2022. **279**(4): p. 1851-1861.

12. Koch, R.W., H.M. Ladak, M. Elfarnawany, and S.K. Agrawal, *Measuring Cochlear Duct Length - a historical analysis of methods and results.* J Otolaryngol Head Neck Surg, 2017. **46**(1): p. 19.

13. Cochlear™, *Reference Guide: Implant Electrode Comparison*.

14. Company, M., *Electrode Arrays: Designed for Atraumatic Implantation Providing Superior Hearing Performance*.

15. Dhanasingh, A. and C. Jolly, *An overview of cochlear implant electrode array designs.* Hear Res, 2017. **356**: p. 93-103.

16. Moran, M., R.C. Dowell, C. Iseli, and R.J.S. Briggs, *Hearing Preservation Outcomes for 139 Cochlear Implant Recipients Using a Thin Straight Electrode Array.* Otol Neurotol, 2017. **38**(5): p. 678-684.

17. Gibson, P. and P. Boyd, *Optimal electrode design: Straight versus perimodiolar.* Eur Ann Otorhinolaryngol Head Neck Dis, 2016. **133 Suppl 1**: p. S63-5.

18. Sennaroglu, L. and M.D. Bajin, *Classification and Current Management of Inner Ear Malformations.* Balkan Med J, 2017. **34**(5): p. 397-411.

19. O'Connell, B.P., R.H. Hunter Jb Fau - Gifford, A. Gifford Rh Fau - Rivas, D.S. Rivas A Fau - Haynes, J.H. Haynes Ds Fau - Noble, G.B. Noble Jh Fau - Wanna, and G.B. Wanna, *Electrode Location and Audiologic Performance After Cochlear Implantation: A Comparative Study Between Nucleus CI422 and CI512 Electrode Arrays.* (1537-4505 (Electronic)).

20. Shepherd, R.K., S. Hatsushika, and G.M. Clark, *Electrical stimulation of the auditory nerve: the effect of electrode position on neural excitation.* Hear Res, 1993. **66**(1): p. 108-20.

21. Alsughayer, L., Y. Al-Shawi, M. Yousef, and A. Hagr, *Cochlear electrode array TFO in incomplete partition-I - A case report.* Int J Pediatr Otorhinolaryngol, 2020. **139**: p. 110438.

22. Sabban, D., M. Parodi, M. Blanchard, V. Ettienne, I. Rouillon, and N. Loundon, *Intra-cochlear electrode TFO.* Cochlear Implants Int, 2018. **19**(4): p. 225-229.

23. Xu, S.A., K.I. McAnally, J. Xu, and G.M. Clark, *Comparison of half-band and full-band electrodes for intracochlear electrical stimulation.* Ann Otol Rhinol Laryngol, 1993. **102**(5): p. 363-7.

24. Jackler, R.K. and W.P. Dillon, *Computed tomography and magnetic resonance imaging of the inner ear.* Otolaryngol Head Neck Surg, 1988. **99**(5): p. 494-504.

25. Cochlear™, *Nucleus® Implants Magnetic Resonance Imaging (MRI) Guidelines*. 2019.

26. MEDEL, *MRT-Hinweise für Cochlea-*Implantate *von MED-EL*. 2018.

27. Breda, A. and A. Territo, *Virtual Reality Simulators for Robot-assisted Surgery.* Eur Urol, 2016. **69**(6): p. 1081-2.

28. Moglia, A., V. Ferrari, L. Morelli, M. Ferrari, F. Mosca, and A. Cuschieri, *A Systematic Review of Virtual Reality Simulators for Robot-assisted Surgery.* Eur Urol, 2016. **69**(6): p. 1065-80.

29. Chen, J.Y., F.J. Seagull, P. Nagy, P. Lakhani, E.R. Melhem, E.L. Siegel, and N.M. Safdar, *Computer input devices: neutral party or source of significant error in manual lesion segmentation?* J Digit Imaging, 2011. **24**(1): p. 135-41.

30. Rogers, B.P., J.M. Sheffield, A.S. Luksik, and S. Heckers, *Systematic Error in Hippocampal Volume Asymmetry Measurement is Minimal with a Manual Segmentation Protocol.* Front Neurosci, 2012. **6**: p. 179.

31. Bruns, N., *[3D Slicer : Universal 3D visualization software].* Unfallchirurg, 2019. **122**(8): p. 662-663.

32. Chen, X., L. Xu, H. Wang, F. Wang, Q. Wang, and R. Kikinis, *Development of a surgical navigation system based on 3D Slicer for intraoperative implant placement surgery.* Med Eng Phys, 2017. **41**: p. 81-89.

33. Hirsch, J.D., R.L. Vincent, and D.J. Eisenman, *Surgical reconstruction of the ossicular chain with custom 3D printed ossicular prosthesis.* 3D Print Med, 2017. **3**(1): p. 7.

34. Cseh, M., Z. Geretovszky, Z. Vereb, and F. Bari, *The 3D (Printing) Center of the University of Szeged: opportunities and challenges*. 2021. 57-57.

35. Dhanasingh, A. and C. Jolly, *Review on cochlear implant electrode array tip fold-over and scalar deviation.* J Otol, 2019. **14**(3): p. 94-100.

36. Meshik, X., T.A. Holden, R.A. Chole, and T.E. Hullar, *Optimal cochlear implant insertion vectors.* Otol Neurotol, 2010. **31**(1): p. 58-63.

37. Ambrose, S.E. and N.W. Todd, Jr., *'Cochlear view' plain radiograph: A simple reliable positioning method.* Cochlear Implants Int, 2018. **19**(2): p. 100-103.

38. Khurayzi, T., F. Almuhawas, A. Alsanosi, Y. Abdelsamad, U. Doyle, and A. Dhanasingh, *A novel cochlear measurement that predicts inner-ear malformation.* Sci Rep, 2021. **11**(1): p. 7339.

39. Braga, J., C. Samir, L. Risser, J. Dumoncel, D. Descouens, J.F. Thackeray, P. Balaresque, A. Oettle, J.M. Loubes, and A. Fradi, *Cochlear shape reveals that the human organ of hearing is sex-typed from birth.* Sci Rep, 2019. **9**(1): p. 10889.

40. Pile, J. and N. Simaan. *Characterization of friction and speed effects and methods for detection of cochlear implant electrode tip fold-over*. in *2013 IEEE International Conference on Robotics and Automation*. 2013.

41. Yilmazer, R.A.-O., E. Karatay, S. Akbulut, Z. Alkan, and B. Sarikaya, *Anatomical landmarks for cochlear implantatıon in ossified cochleas.* (1434-4726 (Electronic)).

42. Cochlear™, *Nucleus® CI632 cochlear implant with Slim Modiolar electrode, Physician's Guide, Canada* https://www.cochlear.com/ifu/documents/d1144283-en-ci632.

43. Pelliccia, P., F. Venail, A. Bonafé, M. Makeieff, G. Iannetti, M. Bartolomeo, and M. Mondain, *Cochlea size variability and implications in clinical practice.* (1827-675X (Electronic)).

44. O'Connell, B.P., J.B. Hunter, and G.B. Wanna, *The importance of electrode location in cochlear implantation.* Laryngoscope Investig Otolaryngol, 2016. **1**(6): p. 169-174.

45. Zuniga, M.G., A. Rivas, A. Hedley-Williams, R.H. Gifford, R. Dwyer, B.M. Dawant, L.W. Sunderhaus, K.L. Hovis, G.B. Wanna, J.H. Noble, and R.F. Labadie, *tip fold-overin Cochlear Implantation: Case Series.* Otol Neurotol, 2017. **38**(2): p. 199-206.

46. Nagy, R., J.A. Jarabin, B. Dimak, A. Perenyi, F. Toth, V. Szuts, J. Jori, J.G. Kiss, and L. Rovo, *[Possibilities for residual hearing preservation with Nucleus CI532 Slim Modiolar electrode array. Case report].* Orv Hetil, 2018. **159**(41): p. 1680-1688.

47. Schieferbein, V., J. Bredemann, R. Schmitt, I. Stenin, T. Klenzner, J. Schipper, and J. Kristin, *Influence of patient-specific anatomy on medical computed tomography and risk evaluation of minimally invasive surgery at the otobasis.* Eur Arch Otorhinolaryngol, 2019. **276**(2): p. 375-382.

48. Aschendorff, A., R. Briggs, G. Brademann, S. Helbig, J. Hornung, T. Lenarz, M. Marx, A. Ramos, T. Stover, B. Escude, and C.J. James, *Clinical investigation of the Nucleus Slim Modiolar Electrode.* Audiol Neurootol, 2017. **22**(3): p. 169-179.

49. Ishiyama, A., F. Risi, and P. Boyd, *Potential insertion complications with cochlear implant electrodes.* Cochlear Implants Int, 2020. **21**(4): p. 206-219.

50. Perenyi, A., Z. Bella, Z. Barath, P. Magyar, K. Nagy, and L. Rovo, *[Role of cone-beam computed tomography in diagnostic otorhinolaryngological imaging].* Orv Hetil, 2016. **157**(2): p. 52-8.

51. Fuchs-Buder, T., N. Settembre, and D. Schmartz, *[Hybrid operating theater]*. Anaesthesist, 2018. **67**(7): p. 480-487.

52. Nollert, G. and S. Wich, *Planning a cardiovascular hybrid operating room: the technical point of view.* Heart Surg Forum, 2009. **12**(3): p. E125-30.

53. Schaadt, J. and B. Landau, *Hybrid OR 101: A Primer for the OR Nurse.* AORN journal, 2013. **97**: p. 81-100.

Társszerzői lemondó nyilatkozat

Alulírott Dr. Perényi Ádám (felelős társszerző) kijelentem, hogy Horváth Bence (pályázó) PhD értekezésének tézispontjaiban bemutatott – közösen publikált – tudományos eredmények elérésében a pályázónak meghatározó szerepe volt, ezért ezeket a téziseket más PhD fokozat megszerzését célzó minősítési eljárásban nem használta fel, illetve nem kívánja felhasználni.

2022.11.14, Szeged

……………………………………
Dr. Perényi Ádám
(szerző)

A pályázó tézispontjaiban érintett, közösen publikálta közlemények:

Perényi Á, Nagy R, Horváth B, Posta B, Dimák B, Csanády M, Kiss JG, Rovó L. Új műtéti képalkotó lehetőség a belsőfül-implantátum elektródasorának dinamikus helyzetmeghatározására [A novel intraoperative imaging tool to follow the cochlear implant electrode array insertion dynamics]. Orv Hetil. 2021 May 30;162(22):878-883.

I.

Az emberi hibatényező vizsgálata CT felvételek manuális kiértékelésekor

Horváth Bence[*,1], Nagy Attila**, Beöthy-Fehér Orsolya[*,2], Rovó László[*,3], Kiss József Géza[*,4]
[*]Szegedi Tudományegyetem, Fül- Orr- Gégészeti és Fej- Nyaksebészeti Klinika, horviratus@gmail.com[1], tsurmo02@gmail.com[2], office.orl@med.u-szeged.hu[3], kjg@orl.szote.u-szeged.hu[4]
6725 Szeged Tisza Lajos krt. 111
[**]Szegedi Tudományegyetem, Orvosi Fizikai és Orvosi Informatikai Intézet, attila@orl.szote.u-szeged.hu
6720 Szeged Korányi fasor 9

Összefoglaló: Öt önkéntes egyetemistának CT felvételeken kellett anatómiai pontokat kijelölni, és vizsgáltuk, hogy a mérési alkalmakkal, hogyan változik a pontosságuk. A kapott mérési eredmények segítenék a témavezetők munkáját, amennyiben ilyen jellegű kutatási témát vezetnek, hogy a hallgató eredményei mennyire relevánsak.

Bevezetés

Fejlődő világunkban egyre nagyobb teret hódít az informatika, ami már az orvostudományokban is meghatározó területet képvisel. A technológia fejlődésével olyan újfajta eljárások születtek, amik segítségével már virtuálisan is megtervezhetők [1], sőt akár el is végezhetők az egyes műtéti eljárások, ezáltal csökkentve az invazív sebészettel járó kockázatot.

Célkitűzés

Munkánk során az emberi hibatényezőt vizsgáltuk, amikor manuálisan kell CT felvételeket kiértékelni. A kapott eredményekből arra szerettünk volna választ kapni, hogy egy laikus vagy pályakezdő felhasználó mennyire tudja pontosan meghatározni, bejelölni az előre megadott anatómiai pontokat. Azért nem radiológusokat választottunk erre a feladatra, mert egyes szakdolgozati munkákhoz is szükséges ilyen jellegű munkának az elvégzése, így fontos tudni, hogy a szakdolgozó eredményei mennyire megbízhatóak. Még fontosabb ez abban az esetben, ha az eredményeket később referencia adathalmazként szeretnénk felhasználni.

Módszer

A vizsgálatra öt önkétes egyetemistát kértünk fel, akiknek a 3D Slicer ingyenesen hozzáférhető orvosi képfeldolgozó programmal [2,3] kellett három különböző korú (1, 4 és 27 éves) páciens koponya CT felvételein anatómiai pontokat (1. táblázat) kijelölni. A pontokat három különböző napon határozták meg és minden képet alkalmanként ötször értékeltek ki. Így az egy adott pontról képenként 15 mérési adat állt rendelkezésünkre minden hallgató esetében. A hallgatók a mérések elvégzése előtt oktatást kaptak a szoftver használatáról illetve az anatómiai pontok felismeréséről a CT felvételeken. Az alábbi táblázat foglalja össze a kijelölt pontokat és a számított síkokat:

1. táblázat A kijelölt anatómiai pontok és a belőlük számított síkok

Kijelölt pontok	Számított síkok
Mastoid csúcsok	Axiális síkokok
Axiális félkörös ívjáratok	Sagittalis síkokok
Sagittalis félkörös ívjáratok	Coronalis síkokok
Coronalis félkörös ívjáratok	Mastoid-Orrcsúcs-Rostrum síkok
Orrcsúcs	Orrcsúcs-Rostrum-Inion síkok
Rostrum hátsó pólusa	
Inion	

Vizsgálatink során figyeltük, hogyan változik a mérési alkalmak elteltével a pontok távolsága egy előre megadott referencia pontcsoporthoz képest, valamint a páciensek kora befolyásolja-e a kijelölések pontosságát. Kiszámítottuk a pontok által kijelölt anatómiai síkokat és bezárt szögeiket, amiket szintén összevetettünk egy referencia adathalmazzal. A síkok meghatározásához és a különböző számítási feladatok elvégzésére Matlab programot írtunk.

Eredmények

1. *Mért pontok és referencia pontok közötti távolság*

Mivel a félkörös ívjáratokon kijelölt három pont bárhol lehet az adott síkon, így ezen pontok között távolságot számolni nem érdemes, így csak a pontszerű eseteket vizsgáltuk: mastoid csúcsok mindkét oldalon, orrcsúcs, rostrum hátsó pólusa, inion. Mindhárom korcsoportnál közel azonos eredmények születtek, az életkor nem befolyásoló tényező. A rostrum hátsó pólusán voltak a legpontatlanabbak a mérések, itt körülbelül 20 mm-es eltéréseket is kaptunk. Legjobb eredményt a mastoid csúcsoknál értek el az önkéntesek, ahol szinte nem is volt eltérés a referencia adatokhoz képest. Az 1. ábra szemlélteti az eredményeket, az adatok az egyik személy mérési eredményei, alkalmanként átlagolva.

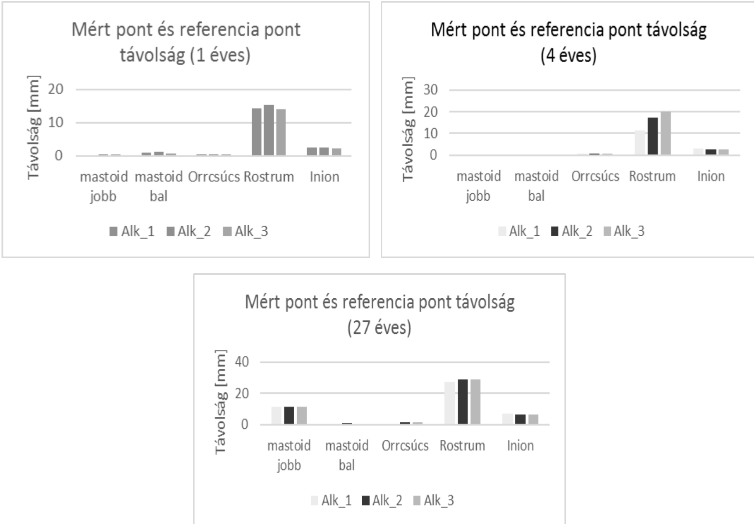

1. ábra A mért és a referncia pontok közötti távolság

2. A számított és a referencia síkok által bezárt szögek

Kiszámítottuk mekkora a bezárt szög a kimért síkok és a referencia síkok között. Az egy pontra jutó méréseket (15 db) összevetettük a referencia adatokkal és ezek összesített átlagát mutatja be a 2. ábra:

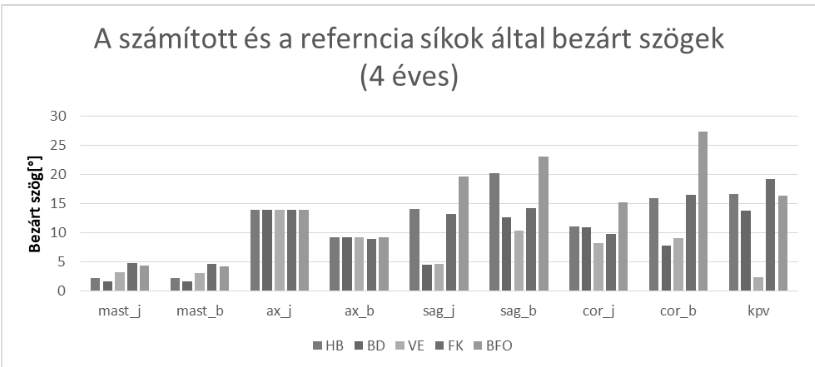

2. ábra A számított és a referencia síkok által bezárt szögek

Ideálisan a bezárt szögnek 0°-nak kellene lennie, ahogy a diagrammon is látható ez nem valósult meg. Átlagosan körülbelül 20°-os eltéréseket tapasztaltunk. A korcsoportok között ismét nincs jelentős különbség.

Ezután kiszámítottuk a síkok által bezárt szögeket és vizsgáltuk mekkora az eltérés a referencia adatokhoz képest. Ezeket az eltéréseket mutatja be a 3. ábra:

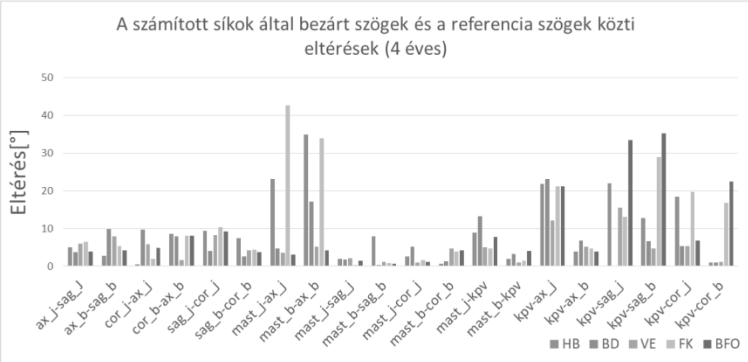

3. ábra A számított síkok által bezárt szögek és a referencia szögek közti eltérések

Többségében 10°-os vagy kisebb eltérések tapasztaltunk, vagyis nem valósult meg a 0°-s különbség. A legnagyobb eltérések a mastoid-axiális síkok és a középvonal-sagittalis síkok között voltak, itt 30°-nál nagyobb eltérések is születtek. Minhárom korcsoportnál közel azonos eredmények születtek.

Következtetések

Összességében elmondható, hogy az önkéntesek még nem elég pontosak számos pont és sík tekintetében. A legnagyobb eltéréseket a félkörös ívjáratoknál tapasztaltuk, ami azzal magyarázható, hogy nagyon kis térfogatokat kellet megjelölni és ilyen dimenziókban már akár 1 mm-es tévedés is nagy eltéréseket tud okozni. Ezt a problémát esetleg további mérési alkalmakkal, illetve egy még részletesebb oktatással lehetne orvosolni.

Hivatkozások

[1] Vannier M.W., Marsh J.L., Warren J.O., "Three Dimensional CT Reconstruction Images for Craniofacial Surgical Planning and Evaluation". Radiology. 150 (1): 179–84. doi:10.1148/radiology.150.1.6689758; 1984
[2] Fedorov A., Beichel R., Kalpathy-Cramer J., Finet J., Fillion-Robin J-C., et al., 3D Slicer as an Image Computing Platform for the Quantitative Imaging Network. Magnetic Resonance Imaging; 30(9):1323-41. PMID: 22770690; 2012 Nov
[3] https://www.slicer.org

II.

A NEW METHOD TO DETERMINE THE OPTIMAL ORIENTATION OF SLIM MODIOLAR COCHLEAR IMPLANT ELECTRODE ARRAY INSERTION

HORVÁTH Bence[1, 2], PERÉNYI Ádám[2], MOLNÁR Fiona Anna[3], CSANÁDY Miklós[2], KISS József Géza[2], ROVÓ László[2]

[1]University of Szeged, Doctoral School of Clinical Medicine, Szeged
[2]University of Szeged, Department of Oto-Rhino-Laryngology and Head-Neck Surgery, Szeged
[3]University of Szeged, Faculty of Medicine, Szeged

English | https://doi.org/10.18071/isz.74.0191 | www.elitmed.hu

Background and purpose – Our goal was to determine the optimal orientation of insertion of the Slim Modiolar electrode and develop an easy-to-use method to aid implantation surgery. In some instances, the electrode arrays cannot be inserted in their full length. This can lead to buckling, interscalar dislocation or tip fold-over. In our opinion, one of the possible reasons of tip fold-over is unfavourable orientation of the electrode array. Our goal was to determine the optimal orientation of the Slim Modiolar electrode array relative to clear surgical landmarks and present our method in one specified case.
Methods – For the measurement, we used the preoperative CT scan of one of our cochlear implant patients. These images were processed by an open source and free image visualization software: 3D Slicer. In the first step we marked the tip of the incus short process and then created the cochlear view. On this view we drew two straight lines: the first line represented the insertion guide of the cochlear implant and the second line was the orientation marker (winglet). We determined the angle enclosed by winglet and the line between the tip of the incus short process and the cross-section of previously created two lines. For the calculation we used a self-made python code.
Results – The result of our algorithm for the angle was 46.6055°. To validate this result, we segmented, from the CT scan, the auditory ossicles and the membranaceous labyrinth. From this segmentation we generated a 3D reconstruction. On the 3D view, we can see the position of

ÚJ MÓDSZER A VÉKONY PERIMODIOLÁRIS COCHLEARIS IMPLANTÁTUMELEKTRÓDA IDEÁLIS BEVEZETÉSI IRÁNYÁNAK MEGHATÁROZÁSÁRA
Horváth B, Perényi Á, MD; Molnár FA, Csanády M, MD; Kiss J, MD, PhD; G, MD, PhD; Rovó L, MD, PhD
Ideggyogy Sz 2021;74(5–6):191–195.

Háttér és cél – Célunk az volt, hogy meghatározzuk a vékony perimodioláris elektróda bevezetésének optimális irányát a műtéti orientációt segítő anatómiai struktúrákhoz képest, és könnyen használható módszert dolgozzunk ki az implantátum műtétjének segítésére. Bizonyos esetekben az elektródasor a cochleán belül visszafordul. Véleményünk szerint ennek a problémának az egyik lehetséges oka az elektródasor kedvezőtlen bevezetési iránya. Módszerünket egy kiválasztott speciális eseten mutatjuk be.
Módszerek – A méréshez az egyik cochlearis implantátummal ellátott betegünk preoperatív CT-felvételét használtuk. A felvételt egy nyílt forráskódú és ingyenesen használható képmegjelenítő szoftverrel, a 3D Slicerrel dolgoztuk fel. A mérési módszer kezdeti lépése az üllő rövid nyúlványa csúcsának a kijelölése. Ezután létre kell hozni a cochlearis nézetet, és ezen a nézeten két egyenes vonalat berajzolni: az első vonal az elektródasor vezetőjét, a második vonal az orientációs jelzőt jelenti. A meghatározni kívánt szög az orientációs jelző és az üllő rövid nyúlványát a korábban felvitt egyenesek metszéspontjával összekötő egyenes által bezárt szög. A számításhoz egy saját python kódot használtunk.
Eredmények – Az algoritmusunk eredménye 46,605° volt. Ennek validálásához a hallócsontokat és a hártyás labirintust kiszegmentáltuk a CT-felvételből, majd ebből készítettünk egy 3D-s modellt, amelyben láthatjuk az előző vonalak helyzetét az anatómiai struktúrákhoz képest. Ezután elforgattuk a 3D-s modellt a vonalakkal

Correspondent: HORVÁTH Bence, Szegedi Tudományegyetem, Szent-Györgyi Albert Klinikai Központ, Fül-orr-gégészeti és Fej-nyaksebészeti Klinika; 6723 Szeged, Gyöngyvirág u. 20/B, 8.em./24.
Telefon: +36302962766, e-mail: h256426@stud.u-szeged.hu
https://www.orcid.org/0000-0002-8367-4259

Érkezett: 2021. február 1. Elfogadva: 2021. április 29.

the previous lines relative to the anatomical structures. After this we rotated the 3D model together with the lines so that the insertion guide forms a dot. In this view, the angle was measured with ImageJ and the result was 46.599°.
Conclusion – We found that our method is easy, fast, and time-efficient. The surgery can be planned individually for each patient, based on their routine preoperative CT scan of the temporal bone, and the implantation procedure can be made safer. In the future we plan to use this method for all cochlear implantation surgeries, where the Slim Modiolar electrode is used.

Keywords: *cochlear implantation, surgery planning, image processing, tip-fold over, Slim Modiolar*

együtt, hogy az elektródasor vezetője pontként ábrázolódjon. A szöget ImageJ-jel megmérve az eredmény 46,599° lett.
Következtetés – Megállapítottuk, hogy módszerünk egyszerű, gyors és időhatékony. A műtétet minden beteg számára egyedileg lehet megtervezni a műtét előtt készített CT-felvétel alapján, és segítségével biztonságosabbá tehető a vékony perimodioláris elektróda implantációja. A jövőben tervezzük, hogy minden vékony perimodioláris elektródával folytatott műtét előtt elvégezzük a méréseket, ezáltal növelve az implantáció sikerességét.

Kulcsszavak: *cochlearis implantáció, műtéti tervezés, képfeldolgozás, tip-fold over, Slim Modiolar*

Cochlear implantation is an effective hearing rehabilitation technique for patients with severe-to-profound sensorineural hearing loss[1]. The spiral ganglion cells are directly stimulated by electrical signals that are transmitted via an electrode array that is surgically inserted into the cochlea. This can lead to buckling, interscalar dislocation or tip-fold over[2–5]. Another possible hazard is short circuiting and implant loss.

The highest proportion of the cochlear implants (CI) that were implanted at the Department of Otorhinolaryngology, Head and Neck Surgery, University of Szeged were Cochlear™ Nucleus® CI532 and CI632 since 2015. Both devices are mounted with one of the thinnest perimodiolar electrode arrays (Slim Modiolar)[6]. Periomodiolar means that the electrode array is pre-curved and this property predisposes its close-to-modiolus or modiolus hugging position. The reason our team has preferred this specific electrode array is: its potential to be superior to the thicker Contour Advance and straight electrode with regards to proximity to the modiolus; lower energy consumption for stimulation and less trauma to the cochlea[7–10]. On the other hand, although easy after proper training, the insertion procedure can be challenging[11]. An adverse event, tip fold-over of the Slim Modiolar electrode, has been reported with higher incidence than with other electrodes.

In our opinion, one of the possible reasons of tip fold-over is unfavourable orientation of the electrode array. Thus, proper orientation of the electrode during insertion can be considered a possible method of prevention of tip fold-over. Our goal was to determine the optimal orientation of the Slim Modiolar array relative to clear surgical landmarks and present our method in one selected case.

Methods

For the measurement, we used the preoperative CT scan (slice thickness 0.6 mm, no gap, bone kernel) of one of our cochlear implant patients. Selection criteria were good quality high-resolution CT scan of the temporal bones, without a reported anatomical malformation and uncomplicated cochlear implantation with a perimodiolar (Cochlear™ Slim Modiolar) electrode array. The good quality of the CT scan and the normal anatomy of the selected 70-year-old male subject was confirmed by a radiologist who obtained subspecialisation in head and neck imaging. These images were processed by an open source and free image visualization software: 3D Slicer (version: 4.10.1, operating system Win10)[12–14], that is available on all platforms (Win, Mac, Linux). This software is able to read many image file formats, including DICOM. After having imported the DICOM files, we converted the image series into single ".nrrd" files, the proprietary file format of 3D Slicer. By doing this conversion process, 3D Slicer anonymizes the images, after which the images do not contain any personal information on the patient.

In our case study we present our semi-automatic algorithm to perform the measurements related to visible surgical landmarks.

In the first step, the user created the cochlear view (Plane A)[15]. The basal turn of the cochlea is best seen in one special plane, i.e. the cochlear view. This plane can be easily created by rotating the coronal plane. The plane of the cochlear view is practically the plane of the proper electrode insertion.

Subsequently, the user created two straight lines: the first line represented the insertion guide of the

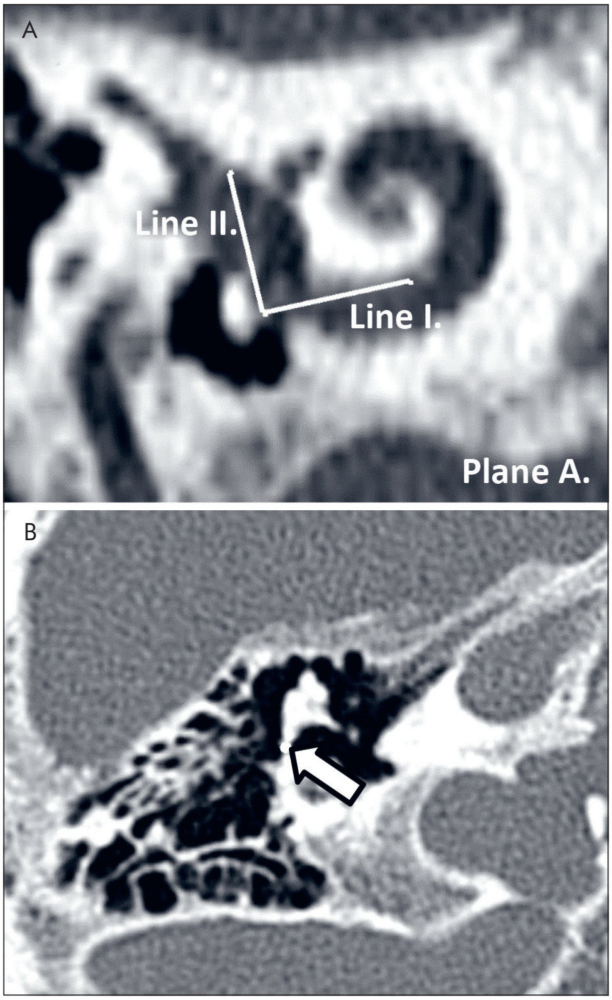

Figure 1. A. *The cochlear view of the right cochlea (Plane A), and the lines defined as Line I. (insertion guide) and Line II. (orientation marker, called winglet),* **B.** *the tip of the incus short process on the axial plane in the right temporal bone (arrow)*

cochlear implant (Line I.) and the second line the orientation marker (winglet, Line II.) shown in **Figure 1.A**. These two lines are perpendicular to each other and intersect at the round window. Finally, the user marked the tip of the short process of the incus **(Figure 1.B)**. The incus short process was depicted on the CT scan and was connected with the cross-section of the winglet and the insertion guide. This is the line to which we compare the position of the winglet.

The above mentioned three parameters are sufficient to calculate the optimal angle of the orientation marker. We determined the angle enclosed by Line II. and the line between the tip of the incus short process and the cross-section of Line I. and Line II. This third (virtual) line is coded as Line III. Although the surgeon is able to visualize the depth (3D view) with the surgical microscope, estimation of angles and planning the surgery is easier and more accurate in one plane (2D view). For this reason, we projected Line I. and Line II. onto one common plane (Plane B). This plane is perpendicular to the Plane A Line I., and parallel with Line II. **(Figure 2)**.

Plane B will be outside the real surgical view. Nevertheless, we do not need to move the Plane B (projection plane) into the view of the surgery, because the projection does not change the measured angle. For this mathematic problem, we wrote an algorithm in python (Python 3), to quantify the angle enclosed between these lines in degrees.

Results

The good quality of the CT scan of the right temporal bone was confirmed by a trained head and neck radiologist. The radiologist also confirmed that the temporal bone was free of anatomical malformation, which was consistent with the official radiologist's report. Each step by the user (determination of the landmarks, lines and planes) was approved by the radiologist. The postoperative radiography showed unremarkable position of the electrode inside the cochlea **(Figure 3.A)**. On **Figure 3.B** is shown a microscopic view with the landmarks (incus short process, round window) and the electrode array with the insertion sheath. The result of our algorithm for the angle between the projected lines (incus–round window and insertion direction) was 46.605 degrees. To validate this result, with 3D Slicer we segmented the auditory ossicles and the

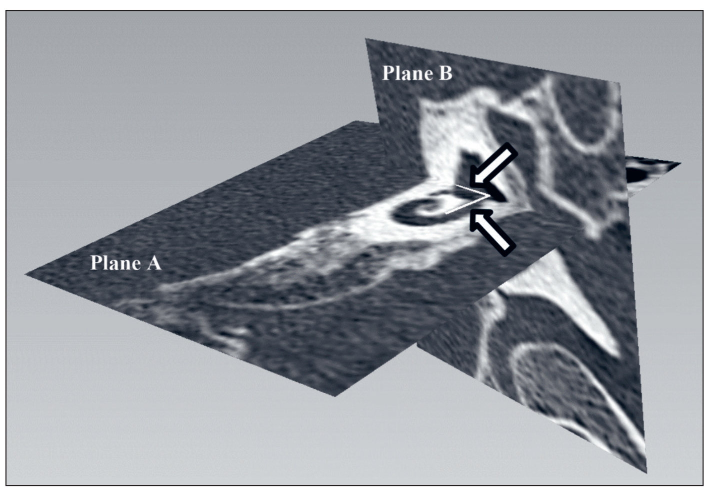

Figure 2. *Plane A: the cochlear view of the right cochlea with the drawn lines (Line I. and Line II.) as shown by arrows, Plane B: the projection plane that contains the line of the orientation marker (Line II.). The user projected the reference line onto Plane B*

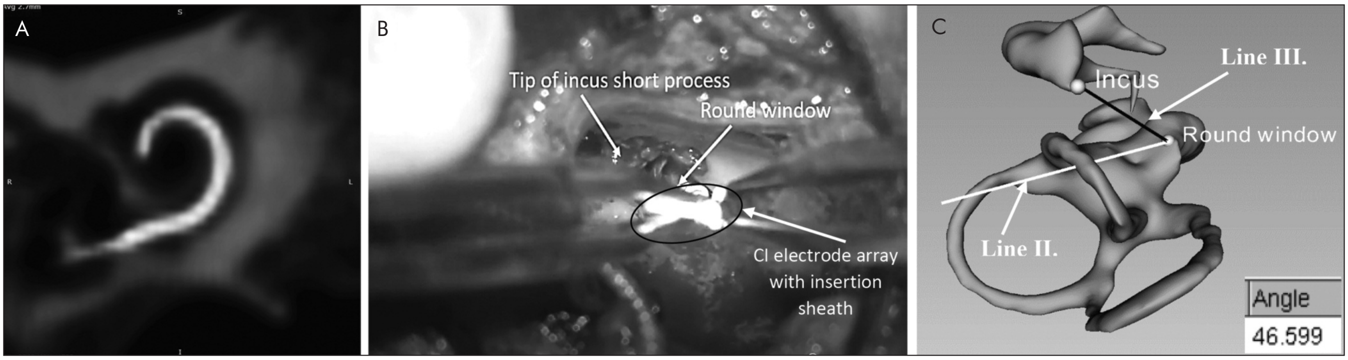

Figure 3. A. *Postoperative 3D volume tomography of the inserted electrode, reconstruction in the cochlear view.* **B.** *The microscopic view through the posterior tympanotomy to the landmarks (incus short process, round window) and orientation of the electrode array with the insertion sheath.* **C.** *3D model of the auditory ossicles (i.e. incus, malleus and anterior crus of stapes) and the membranaceous labyrinth. Black line: reference line (Line III.), white line: orientation marker (Line II.), the angle (measured with ImageJ) was approx. 47 degrees*

membranaceous labyrinth (on CT the liquid and air are hypodense). From this segmentation, we generated a 3D reconstruction. On the 3D view we can see the position of the lines, as shown previously on **Figure 1.A** and **Figure 2** (Line I., Line II.) relative to the anatomical structures **(Figure 1.B)**. Afterwards, we rotated the 3D model together with the lines (Line I., Line II. and Line III.) so that the insertion guide (Line I.) forms a dot as shown in **Figure 3.C**. In this view the angle was measured with ImageJ and the result was 46.599°.

Discussion

Our goal was to determine the optimal orientation of insertion of the Slim Modiolar electrode and develop an easy-to-use method to aid implant planning and surgery. Reference structures that can be clearly visualized during surgery and clearly noticed on the CT image, are essential. The short process of the incus and the round window were chosen as clear anatomical landmarks, due to their nature of visibility during routine cochlear implant surgery via posterior tympanotomy. The surgeon is able to detect these landmarks and relate the position of the electrode array to them. With this measurement tool we aimed to effectively prevent electrode tip fold-over[2, 4, 5], a relatively common adverse event from Slim Modiolar electrode. We assume that a possible reason of tip fold-over is unfavourable orientation of electrode during insertion. Other reasons include the various anatomical structure of cochlea, for example: size, orientation, length, and malformations[16], so it is necessary to individually plan the surgery beforehand.

In this paper we presented a new method to determine the optimal insertion angle of the Slim Modiolar cochlear implant electrode. We found that our method is easy, fast, and time-efficient. The surgery can be planned individually for each patient based on their routine preoperative CT scan of the temporal bone and the implantation procedure can be made more safe. In the future, we plan to use this method for all cochlear implantation surgeries, where the Slim Modiolar electrode was used.

REFERENCES

1. *Clark GM*. The multiple-channel cochlear implant: the interface between sound and the central nervous system for hearing, speech, and language in deaf people-a personal perspective. Philos Trans R Soc Lond B Biol Sci 2006; 361(1469):791-810. https://doi.org/10.1098/rstb.2005.1782
2. *Zuniga MG, Rivas A, Hedley-Williams A, Gifford RH, Dwyer R, Dawant BM, et al*. Fold-over in cochlear implantation: Case series. Otol Neurotol 2017;38(2):199-206. https://doi.org/10.1097/MAO.0000000000001283
3. *Dimak B, Nagy R, Perenyi A, Jarabin JA, Schulcz R, Csanady M, et al*. Review of electrode placement with the Slim Modiolar Electrode: identification and management. Ideggyogy Sz 2020;73(1-2):53-9. https://doi.org/10.18071/isz.73.0053
4. *Ramos-Macias A, Falcon-Gonzalez JC*. Mechanisms of electrode fold-over in cochlear implant surgery when using a flexible and slim perimodiolar electrode array. Acta Otolaryngol 2017;137(11):1129-35. https://doi.org/10.1080/00016489.2016.1271449
5. *Sabban D, Parodi M, Blanchard M, Ettienne V, Rouillon I,*

Loundon N. Intra-cochlear electrode tip fold-over. Cochlear Implants Int 2018;19(4):225-9.
https://doi.org/10.1080/14670100.2018.1427823
6. *Gstoettner WK, Adunka O, Franz P, Hamzavi J, Plenk H, Susani M, et al.* Perimodiolar electrodes in cochlear implant surgery. Acta Otolaryngol 2001;121(2):216-9.
https://doi.org/10.1080/000164801300043569
7. *Perenyi A, Toth F, Dimak B, Nagy R, Schoerg P, Jori J, et al*. Electrophysiological measurements with electrode types of different perimodiolar properties and the same cochlear implant electronics - a retrospective comparison study. J Otolaryngol Head Neck Surg 2019;48(1):46.
https://doi.org/10.1186/s40463-019-0361-8
8. *Roland PS, Wright CG*. Surgical aspects of cochlear implantation: mechanisms of insertional trauma. Adv Otorhinolaryngol 2006;64:11-30.
https://doi.org/10.1159/000094642
9. *Skarzynski H, Matusiak M, Lorens A, Furmanek M, Pilka A, Skarzynski PH*. Preservation of cochlear structures and hearing when using the Nucleus Slim Straight (CI422) electrode in children. J Laryngol Otol 2016; 130(4):332-9.
https://doi.org/10.1017/S0022215115003436
10. *Adunka OF, Pillsbury HC, Kiefer J*. Combining perimodiolar electrode placement and atraumatic insertion properties in cochlear implantation - fact or fantasy? Acta Otolaryngol 2006;126(5):475-82.
https://doi.org/10.1080/00016480500437393
11. *Dhanasingh A*. Why pre-curved modiolar hugging electrodes only cover the basal turn of the cochlea and not beyond that? J Int Adv Otol 2018;14(3):376-81.
https://doi.org/10.5152/iao.2018.5831
12. *Bruns N*. 3D Slicer: Universal 3D visualization software. Unfallchirurg 2019;122(8):662-3.
https://doi.org/10.1007/s00113-019-0654-4
13. *Fedorov A, Beichel R, Kalpathy-Cramer J, Finet J, Fillion-Robin JC, Pujol S, et al.* Kikinis, 3D Slicer as an image computing platform for the Quantitative Imaging Network. Magn Reson Imaging 2012;30(9):1323-41.
https://doi.org/10.1016/j.mri.2012.05.001
14. *Nagy A, Ódor B, Beöthy FO, Perényi Á, Rovó L, Kiss J*. A sziklacsont elhelyezkedésének változása a koponyán belül a gyermekkor során. Fül-Orr-Gégegyógyászat 2017;63(3):154.
15. *Ambrose SE, Todd Jr*. Cochlear view plain radiograph: A simple reliable positioning method. Cochlear Implants Int 2018;19(2):100-3.
https://doi.org/10.1080/14670100.2017.1382757
16. *Sennaroglu L, Bajin MD*. Classification and current management of inner ear malformations. Balkan Med J 2017;34 (5):397-411. https://doi.org/10.4274/balkanmedj.2017.0367

III.

European Archives of Oto-Rhino-Laryngology (2022) 279:5631–5638
https://doi.org/10.1007/s00405-022-07421-8

OTOLOGY

A new method of preoperative assessment of correct electrode array alignment based on post-operative measurements in a cochlear implanted cohort

Bence Horvath[1,2] · Adam Perenyi[2] · Fiona Anna Molnar[3] · Roland Nagy[2] · Miklos Csanady[2] · Jozsef Geza Kiss[2] · Laszlo Rovo[2]

Received: 22 November 2021 / Accepted: 25 April 2022 / Published online: 21 June 2022

Abstract

Purpose During cochlear implantation surgery, a range of complications may occur such as tip fold-over. We recently developed a method to estimate the insertion orientation of the electrode array. The aim of the study was to determine the optimal angle of orientation in a cohort of cochlear implanted patients.

Methods On eighty-five CT scans (80 uncomplicated insertions and 5 cases with tip fold-over), location of the electrode array's Insertion Guide (IG), Orientation marker (OM) and two easily identifiable landmarks (the round window (RW) and the incus short process (ISP)) were manually marked. The angle enclosed by ISP-RW line and the Cochlear™ Slim Modiolar electrode array's OM line determined the electrode array insertion angle.

Results The average insertion angle was 45.0–47.2° ± 10.4–12° SD and was validated with 98% confidence interval. Based on the measurements obtained, patients' sex and age had no impact on the size of this angle. Although the angles of the tip fold-over cases (44.9°, 46.9°, 34.2°, 54.3°, 55.9°) fell within this average range, the further it diverted from the average it increased the likelihood for tip fold-over.

Conclusion Electrode array insertion in the individually calculated angle relative to the visible incus short process provides a useful guide for the surgeon when aiming for the optimal angle, and potentially enhances good surgical outcomes. Our results show that factors other than the orientation angle may additionally contribute to failures in implantation when the Slim Modiolar electrode is used.

Keywords Cochlear implant · Slim Modiolar · Medical image processing · 3D Slicer · Neuro-otology surgery

Abbreviations

CI	Cochlear implant
CT	Computed Tomography
IG	Insertion Guide
ISP	Incus short process
OM	Orientation marker
RW	Round window
SD	Standard deviation

✉ Bence Horvath
horvath.bence.3@stud.u-szeged.hu

1 Doctoral School of Clinical Medicine, University of Szeged, Szeged, Hungary

2 Department of Oto-Rhino- Laryngology and Head- Neck Surgery, University of Szeged, Szeged, Hungary

3 Faculty of Medicine, University of Szeged, Szeged, Hungary

Introduction

Cochlear implantation is a modern and effective hearing rehabilitation technique for patients with severe to profound sensorineural hearing loss [1]. The speech processor, which is worn behind the ear, detects sound and converts it into an electrical signal. The internal unit is implanted surgically to position the stimulating electrodes close to the spiral ganglion cells in the cochlea and directly stimulate them with these electrical signals. The most common procedure to advance the electrode array into the scala tympani of the cochlea is performed by the posterior tympanotomy, by opening the facial recess, via the round window (RW). The bony overhang that restricts the access to the RW membrane is usually removed. The RW anatomy is variable among individuals which in some instances requires its widening ("extended RW approach") [2]. Possible complications of electrode array insertion are interscalar dislocation and tip fold-over [3]. Potential further hazards are formation of short circuits and implant dysfunction. Using the recommended cochlear implant soft surgery techniques [4], it is possible to preserve residual hearing and this would require the preservation of the internal structure of the cochlea.

The highest proportion of the cochlear implants (CI) that were used since 2015 at the Department of Otorhinolaryngology, Head and Neck Surgery, University of Szeged, based on preferable low-trauma procedure and audiological benefits [5] have been Cochlear™ Nucleus® CI532 (Fig. 1.) and CI632. Both devices are mounted with one of the thinnest perimodiolar electrode arrays (Slim Modiolar) [6]. Perimodiolar electrode arrays are pre-curved and this property supports their close-to-modiolus or 'modiolus hugging' position. In our clinic, the perimodiolar electrode array is preferred over the straight and the thicker Contour Advance arrays because of the lower energy consumption for stimulation and less trauma to the cochlea [7]. However, tip fold-over of the Slim Modiolar electrode has been reported with a higher incidence than for any other electrode arrays [8]. One of the possible reasons for tip fold-over is the unfavourable orientation of the electrode array adopted during insertion [8].

The aim of the study was to determine the ideal angle of orientation by calculating the proximity of the electrode array to intraoperatively visible anatomical landmarks, visualised by CT scan, in a cohort of cochlear implanted patients.

Materials and methods

All patients who had severe to profound hearing loss and received cochlear implantation with a Slim Modiolar device (Cochlear™) between January 2016 and September 2021 (Table 1) were included in this study. Ethical approval was obtained from the local ethical research committee, University of Szeged, Szent-Györgyi Albert Medical Center, Regional and Institutional Human Biomedical Research Ethics Committee (Szegedi Tudományegyetem, Szent Györgyi Albert Klinikai Központ Humán Orvosbiológiai Regionális és Intézmenyi Kutatásetikai Bizottság) and the appropriate informed consent was obtained from patient or guardian. Our inclusion criteria of CT scans included: good quality high-resolution CT scans of the temporal bones and clear visible structure of the cochlea and auditory ossicles (high-resolution thin slices up to 0.625 mm, with no motion artefact). Exclusion criteria were cochlear malformations [9], cochlear ossification, and obliterative post meningitis changes. Eighty consecutive CT scans of cochlear implanted patients who underwent uncomplicated implantation with Slim modiolar electrode and complied with the above criteria were analysed to determine the ideal insertion angle. Preoperative CT scans of five patients with electrode array tip fold-over were additionally analysed.

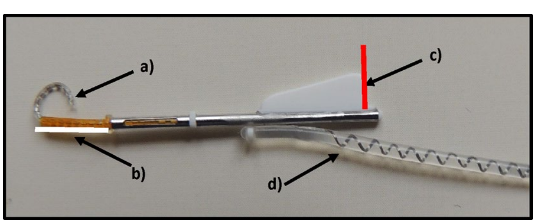

Fig. 1 Cochlear™ Nucleus® CI 532 Slim Modiolar practice cochlear implant. The major parts of the device: **a** Cochlear implant electrode, **b** Insertion Guide (IG; white line), **c** Orientation marker (OM; red line), **d** Electrode lead. These lines (white and red) are marked on the subsequent CT scan (Fig. 2a) and 3D model (Fig. 3a and b) for easier orientation

The required quality of the CT scans and the normal anatomy of the selected patients were confirmed by a radiologist with a subspecialisation in head and neck imaging. These images were processed by an open source free image visualization software: 3D Slicer (version: 4.10.1, operating system Win10) [10], which is available on all platforms (Win, Mac, Linux). After having imported the DICOM files, we converted the image series into single "nrrd" files, the proprietary file format of 3D Slicer. This conversion process anonymized the images, after which the images did not contain any personal information of the patients. This conversion does not introduce distortion or any anomalies into the image.

Calculations were carried out as described in our previous paper [11]. In brief, on cochlear view (Fig. 2a) [12] in which the basal turn of the cochlea is best seen, two straight lines were drawn. The first line represents the insertion guide (IG; white) of the CI and the second line is the orientation marker (OM; red) shown in Fig. 2a. These two lines are perpendicular to each other and intersect at the round window. This view is the plane of the ideal electrode array insertion.

Then the tip of the incus short process (ISP) was marked (Fig. 2b; blue dot) on the axial CT scan and then connected with a virtual line to the round window (ISP-RW, Fig. 3). This line was projected into a common plane with the line of OM. We compared the position of the OM to this ISP-RW virtual line (Fig. 3a; angle α).

The above-mentioned three parameters (lines of IG and OM, ISP) are sufficient to calculate the ideal alignment of the OM and were chosen as measurements, because they are clearly visible during surgery (Fig. 3c and d). The RW was also marked, but its coordinates were not used for the calculations. We created a custom scripted module in 3D Slicer. The 3D coordinates of OM, IG and ISP were loaded into this module to determine the angle enclosed by the line of OM and virtual ISP-RW line. The spatial location of the selected structures during surgery is illustrated in Fig. 3.

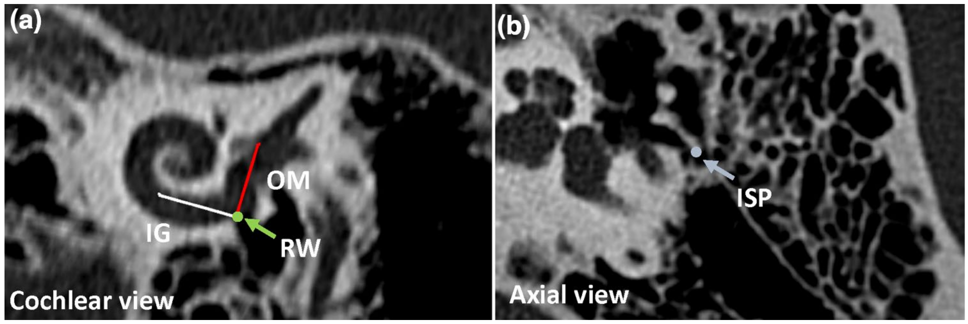

Fig. 2 **a** The lines that represent the parts of the cochlear implants as introduced on Fig. 1: white line: insertion guide (IG), red line: orientation marker (OM). These lines were drawn and cross each other in the round window (RW; green dot). **b** The incus short process (ISP) is indicated on the axial plane (blue)

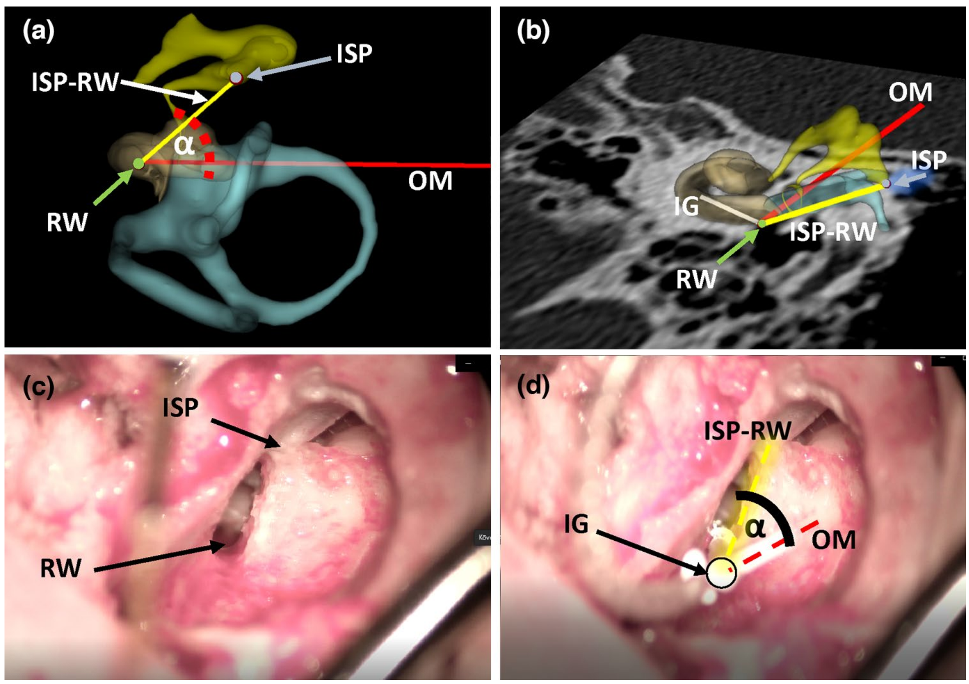

Fig. 3 **a** A 3D model that illustrates the lines and the anatomical structures in the anterior view, α is the calculated angle, in this case $\alpha = 45.07°$. Red line represents OM, yellow line represents the reference ISP-RW line that links the incus short process (ISP) and ends in the round window (RW). IG is perpendicular to the round window. **b** A 3D model in an inferior view, showing the location of each previously mentioned lines on one CT slice (Fig. 2; cochlear view). **c** A surgical image of the view during implantation; the ISP and RW are marked. These are chosen as measurements, because these anatomical landmarks are clearly visible during surgery. **d** The identical surgical image with the CI electrode, IG is closely perpendicular to RW. The line of OM and the line reference ISP-RW are indicated (dashed lines). These lines enclose α, the angle to be determined

Table 1 Distribution of cases by sex and age

	Count	Youngest [years]	Oldest [years]	Average [years]	Standard deviation [years]
Female	36	1	77	24.1	25.4
Male	44	1	75	21.5	24.5
All	80	1	77	22.7	24.8

Results

Basic statistical analysis of the electrode array insertion angles

From eighty different patients, we determined the average angle using our previously developed method [11]. The calculations were performed using our python scripted 3D Slicer module. The results obtained by the program were confirmed by manual measurement of the first five patients' angles (left and right sides). Since the manual

Table 2 Statistical analysis of the measured angles on both sides

	Minimum angle	1st quartile	Median	Mean	3rd quartile	Max. Angle	Standard deviation
Left side	20.5°	34.8°	44.0°	45.0°	53.7°	72.4°	12,0°
Right side	20.9°	40.3°	45.6°	47.2°	53.0°	75.3°	10.4°

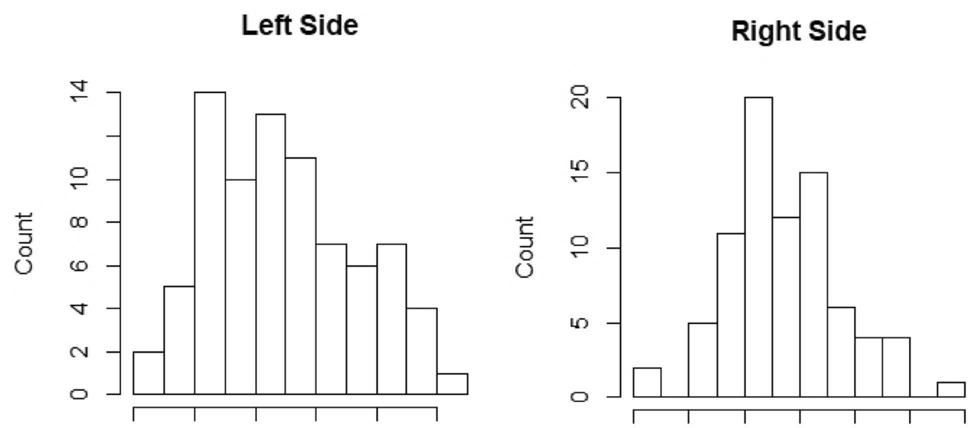

Fig. 4 Histogram of the angle distribution on both sides, mean is 45.0 (left side), 47.2 (right side), standard deviation: 12.0 (left side), 10.4 (right side). We established with Shapiro–Wilk test that the data follow normal distribution, $\alpha = 0.05$, p values: 0.187 (left side), 0.133 (right side)

calculations were equal to the values obtained by the module, we accepted that the program worked correctly. The average age of our cohort was 22.7 years ± 24.8 years SD. The distribution of sex and age when the CT scan was obtained are shown in Table 1.

The ratio of female to male patients in this study was almost 1:1. The youngest participant in this study was 12 months old. A statistical analysis was carried out using a free-to-download statistical function package (R version 3.6.3, IDE: R Studio, Platform: Windows 10) and the results are shown in Table 2.

There was no significant difference between whether the implantation was carried out on the right or the left side. The average angle was close: 45.0–47.2° ± 10.4–12.0° SD (Table 2 and Fig. 4). Afterwards, a 98% confidence interval was calculated for the mean on both sides. On both sides the p value was less than 0.02, thus we can establish that, with 98% probability, the sample mean can represent the population mean. Thus, the expected value of the insertion angle is approximately 45.0–47.2° ± 10.4–12.0° SD.

Correlation of electrode array insertion angle with the side (left or right) of insertion

First, we examined whether there are any linear connections between the left side and right side measurements. For this a Pearson's correlation test was used. It was confirmed that the values of the angles follow a normal distribution, because this is essential when using Pearson's correlation test. For this, we used the Shapiro–Wilk test ($\alpha = 0.05$). On the left side, the p value was 0.187, whereas on the right side, the p value was 0.133 (Fig. 4). Because the p values were higher than 0.05, it was accepted that the angles follow normal distribution. The Pearson's correlation coefficient was 0.513. A significance test was performed for this correlation coefficient. The Student's t distribution value was 5.271 and $t_{78,\,0.05} = 1.99$ ($df = 78$, $\alpha = 0.05$, $p = 1.172e-06$). Because $|t| > t_{78,\,0.05}$ and $p < \alpha$ the correlation coefficient is significantly different from zero, there is a weak positive

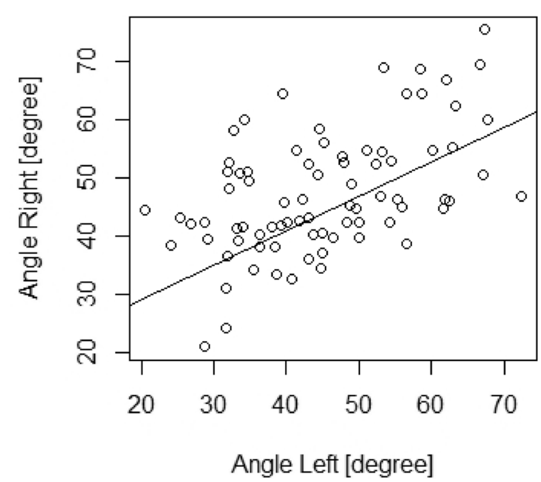

Fig. 5 Scatter plot of the angles, showing a weak positive linear connection between the left and right side measurements (Pearson's correlation coefficient: 0.513) Significance test of the correlation coefficient: coefficient. The Student's t-distribution's t value was 5.271 and $t_{78,\,0.05} = 1.99$ ($df = 78$, $\alpha = 0.05$, $p = 1.172e-06$). Because $|t| > t_{78,\,0.05}$ and $p < \alpha$ the correlation coefficient is significantly different from zero

linear correlation between the measured side and the size of the angle different from zero, which means there is a weak positive linear correlation shown in Fig. 5.

Correlation of electrode array insertion angle with the sex and age of the patients

Previous studies have raised the possibility of the anatomical differences of the cochlea between females and males [13]. We extended our study to compare the different sexes and the size of the electrode array insertion angle. Before a two-sample *t* test the equality of the variance was assessed. The *p* value of the variance test was 0.135 on the left side and 0.084 on the right side ($\alpha = 0.01$). The equality of variance was accepted due to the $p > \alpha$ on both sides. Then a two-sample *t* test was performed which included the angle and the sex of the patient ($\alpha = 0.01$). The *p* value on the left side was 0.124 and on the right side it was 0.115. The *p* values were higher than 0.01, therefore the sex of the patient had no statistically significant effect on the size of the angle.

Then it was examined whether the age of the patient has any effect on the calculated angles. Since age is a discrete variable, a one-way Anova test was used. The *p* value on the left side was 0.712 and on the right side it was 0.160. Because the *p* values were higher than 0.05, indicating that age has no statistically significant effect on the size of the angle.

Electrode array insertion angle in known tip fold-over patients

To compare the electrode array insertion angle in our eighty patients and tip fold-over cases, we determined the insertion angle in five previously implanted patients with confirmed electrode array tip fold-over after the cochlear implantation (Table 3). For this study, preoperative CT scans were used. We then compared the insertion angle where the tip fold-over occurred to the average angle. Although angles of Patient 2 and Patient 3 are very close to the mean, the others (Patient 1, Patient 4 and Patient 5) are close to the endpoint of SD range.

Table 3 Tip fold-over cases

	Left side angle [°]	Right side angle [°]
Patient 1	35.4	**34.2**
Patient 2	**44.9**	37.1
Patient 3	52.9	**46.9**
Patient 4	**54.3**	42.2
Patient 5	**55.9**	44.9

The angles determined in the five patients where tip fold-over occurred. These patients had bilateral cochlear implantations and the angles in bold are the side where the tip fold-over occurred

Discussion

This study investigated the average OM orientation to anatomical landmarks, determined by a custom-made Python script, in eighty cochlear implanted patients' preoperative CT scans. The statistical analysis indicated that the alignment of the electrode array in a successful CI insertion is approximately $45.0° \pm 11°$ SD. Furthermore, there is no impact of the age or the sex of the patients on the insertion angle. However, there was a weak positive linear correlation observed between the left and right sides.

Calculation of insertion angle

3D Slicer software is able to mark anatomical structures, such as the short process of the incus (ISP) on the axial plane of a CT scan. When changed to the coronal plane, it could be rotated to the cochlear view, where the insertion guide (IR) and the orientation marker (OM) could be marked and measured. These 3D points and vectors were loaded into a custom python scripted 3D Slicer module, which was used to calculate the angle. The limitation of this technique is the manual measurements on the CT scans. If the user cannot mark the landmarks or create the exact cochlear view, the angles may be distorted.

With the advancement of imaging techniques and software (e.g. 3D Slicer, RadiAnt DICOM viewer), it is relatively easy to identify anatomical landmarks on a CT scan and calculate the insertion angle. It was previously demonstrated that an anatomical landmark-based approach such as using the centre of the round window at the bony overhang, the basal and apical centre of the modiolus, can be used as a cochleostomy target [14]. This consequently provided valuable information for an image-guided robotic system to carry out the exact surgical drilling based on the estimated optimal trajectory. In this study, the ideal insertion angle of the CI electrode array into the cochlea was identified. However, it would be useful to incorporate the positioning of the cochleostomy that would guide the implant electrode array into the cochlea.

Insertion angle in tip fold-over cases

Until recently, tip fold-over of the electrode array was only small probability (~0,80%) seen in lateral wall electrode arrays. However, with the new thin perimodiolar electrode array model, tip fold-over can occur in ~ 4.7% of cochlear implanted cases [8].

In this study, we calculated that the average angle of the OM to the ISP in successful implantations is approximately 45.0–47.2° ± 10.4–12° SD which was verified with a confidence interval of 98%. Furthermore, after determining the insertion angle on five known tip fold-over cases' preoperative CT scans, the angles did fall within the average range. Although the values suggested that the further the diversion from 45.0° to 47.0° ± SD, the increased chance of tip fold-over. However, in Patient 2 and Patient 3 the measured angles were in the average range, it is possible that the tip fold-over was caused by factors other than the insertion angle alone.

Based on our experience, other contributing factors are likely to include: (i) too fast or forced insertion of the very delicate electrode array [15], (ii) incomplete loading of the array with the tip remaining and curving already outside the IG, (iii) incorrect loading of the electrode array which causes the array to stuck in the slot of the IG, (iv) incorrect insertion trajectory vector, for example, if the array is directed too much towards the medial or lateral wall of the cochlea which also may cause bending of the IG. In this situation, the deformed IG's slot may expand which results in electrode array insertional failure. It is assumed that incorrect insertion trajectory can also be caused by a narrow or insufficiently extended RW or the presence of a pronounced fissula ante-fenestram.

Potential impact and future applications

Anatomical landmark identification during electrode array insertion in CI surgery has been continuously investigated. A study by Meshnik et al. [16] used eight cadaveric human temporal bones and applied a similar technique to our study: the fusion of microCT imaging with Analyze imaging software analysis alongside a custom-written script to determine five possible insertion vectors for the most optimal electrode array site of insertion. However, their study was tailored for cochleostomy approach, therefore, it is not possible to make a direct comparison. The close relationship of the optimal insertion vectors to the facial nerve warrants an investigation to assess whether the optimal angle of orientation identified in this study may also need to take into consideration the location of the facial nerve.

Furthermore, anatomical landmark guidance is becoming important for the future of CI surgery due to technological advancements and improvements in surgical techniques. The CI632 implant user guide [17] lacks a precise numerical recommendation on where the orientation marker should point during the insertion of the electrode array, which may lead to potential misalignment. Our study intended to quantify the optimal position of the orientation marker relative to the visible intraoperative anatomical landmarks. Furthermore, a numerical approach is likely to aid in personalising the electrode array insertion, since the basal turn of the cochlea may vary between individuals. This may also reduce the chance of damaging the basilar membrane by the electrode array, which could result in decreased residual hearing preservation [18]. The use of landmark based and numerical approach is also very valuable for training less experienced surgeons to standardise the process leading to improved consistency through an evidence-based approach [19].

Preserving residual hearing and developing a less traumatic insertion of the electrode array have been main goals for many institutions, which could potentially be achieved using robotic surgery [20–22]. There is limited knowledge on post-robotic insertion hearing outcomes, but recent studies have shown that the robot itself is able to decrease the involuntary movements such as tremor; creates a smooth insertion and the translocated electrodes were decreased in comparison to manual insertion with reduced intracochlear damage, however, navigation and preoperative planning are still under refinement. The optimal angle of orientation identified in the current study, together with the anatomical reference points for electrode array with proven consistent clinical outcomes, could aid the development of preoperative input data for personalised robotic array insertion.

Conclusion

Due to the differences in the individual anatomy, this ~ 45.0°–47.0° ± SD angle range should not be applied automatically for all cases. Although there is a weak positive correlation between the values of left and right side angles, it is necessary to take measurements bilaterally if both sides are implanted. Although this method was developed for the Slim Modiolar electrode, this method could be adopted to other electrode arrays with half-band electrodes (e.g. the Cochlear™ Nucleus® Slim Straight and Contour Advance). If half-band electrodes are used, the position of the OM related to the position of the modiolus should be considered and the calculated angle should be corrected accordingly (e.g. 180° should be added if the marker or guidewire is to be positioned caudally). The full-band electrode types, however, do not require such measurements, because their design allows their insertion in any orientation angle (e.g. MEDEL®: FORM® and CLASSIC® Series). Our results can serve as valuable additional information for the surgeon in planning and performing the implantation procedure. During electrode array insertion, the plane of the basal turn of the cochlea is not visible. The 3D models and the calculated angles provide deeper knowledge of the individual anatomy pre-operatively. Before the insertion of the electrode array into the RW, the surgeon can align the OM towards the ISP using the patients' preoperative calculated angle. This angle considers the individual anatomy of the patient and guides the surgeon based on visible anatomical landmarks. Thus, using the quantified angle, the surgeon does not have to rely exclusively on intuition of the cochlear basal turn during orientation. Furthermore, consideration of cochlear anatomy during electrode array orientation potentially reduces complications such as tip fold-over and interscalar dislocation.

Author contributions BH—performed image processing with 3D Slicer, wrote the python scripted module, performed statistical analysis, prepared the manuscript for publication. AP—analysed the imaging studies, performed intraoperative imaging, controlled the reference points and the measurements, rendered scientific guidance, prepared the manuscript for publication. BH and AP contributed equally, they are shared co-first authors. FM—language proofreading, prepared the manuscript for publication. RN—language proofreading, prepared the manuscript for publication. MC—performed the cochlear implantations, prepared the manuscript for publication for publication. JGK—rendered scientific guidance, supervised the scientific content of the research, finalised the manuscript for publication. LR—Head of the implantation team; performed the cochlear implantations; supervised the scientific content of the research, finalised the manuscript for publication.

Funding Open access funding provided by University of Szeged. The authors declare there is no funding to disclose. The research was supported by University of Szeged Open Access Fund (Grant 5552).

Availability of data and materials The datasets used and/or analysed during the current study are available from the corresponding author on reasonable request.

Code availability Not applicable.

Declarations

Conflict of interest The authors declare that they have no conflict of interest.

Ethics approval and consent to participate All procedures performed in studies involving human participants were in accordance with the ethical standards of the institutional and/or national research committee. Details of the ethical authorization: permit number: 4929, registration number: 15/2021/SZTERKEB, date: 2021.03.22.

Consent for participate Not applicable.

Consent for publication Not applicable.

References

1. Deep NL, Dowling EM, Jethanamest D, Carlson ML (2019) Cochlear implantation: an overview. J Neurol Surg B Skull Base 80(2):169–177
2. Klabbers TM, Heutink F, Huinck WJ, van der Woude WJ, Verbist BM, Mylanus EAM (2022) Intracochlear electrode array position and cochlear implant outcomes using the nucleus Slim Modiolar electrode and the extended round window approach: a follow-up study. Eur Arch Otorhinolaryngol. https://doi.org/10.1007/s00405-021-07247-w
3. Zuniga MG, Rivas A, Hedley-Williams A, Gifford RH, Dwyer R, Dawant BM, Sunderhaus LW, Hovis KL, Wanna GB, Noble JH, Labadie RF (2017) Tip fold-over in cochlear implantation: case series. Otol Neurotol 38(2):199–206
4. Eshraghi AA, Nazarian R, Telischi FF, Rajguru SM, Truy E, Gupta C (2012) The cochlear implant: historical aspects and future prospects. Anat Rec 295(11):1967–1980
5. Perenyi A, Toth F, Dimak B, Nagy R, Schoerg P, Jori J, Kiss JG, Sprinzl G, Csanady M, Rovo L (2019) Electrophysiological measurements with electrode types of different perimodiolar properties and the same cochlear implant electronics—a retrospective comparison study. J Otolaryngol Head Neck Surg 48(1):46
6. McJunkin JL, Durakovic N, Herzog J, Buchman CA (2018) Early outcomes with a slim, Modiolar cochlear implant electrode array. Otol Neurotol 39(1):e28–e33
7. Shaul C, Weder S, Tari S, Gerard JM, O'Leary SJ, Briggs RJ (2020) Slim, Modiolar cochlear implant electrode: melbourne experience and comparison with the contour perimodiolar electrode. Otol Neurotol 41(5):639–643
8. Dhanasingh A, Jolly C (2019) Review on cochlear implant electrode array tip fold-over and scalar deviation. J Otol 14(3):94–100
9. Halawani RT, Dhanasingh A (2020) New classification of cochlear hypoplasia type malformation: relevance in cochlear implantation. J Int Adv Otol 16(2):153–157
10. Bruns N (2019) 3D Slicer: universal 3D visualization software. Unfallchirurg 122(8):662–663
11. Horváth Bence PÁ, Anna MF, Miklós C, Géza KJ, László R (2021) A new method to determine the optimal orientation of Slim Modiolar cochlear implant electrode array insertion. Clin Neurosci 74(5–6):191–195
12. Ambrose SE, Todd NW Jr (2018) "Cochlear view" plain radiograph: a simple reliable positioning method. Cochlear Implants Int 19(2):100–103
13. Braga J, Samir C, Risser L, Dumoncel J, Descouens D, Thackeray JF, Balaresque P, Oettle A, Loubes JM, Fradi A (2019) Cochlear shape reveals that the human organ of hearing is sex-typed from birth. Sci Rep 9(1):10889
14. Wimmer W, Venail F, Williamson T, Akkari M, Gerber N, Weber S, Caversaccio M, Uziel A, Bell B (2014) Semiautomatic cochleostomy target and insertion trajectory planning for minimally invasive cochlear implantation. Biomed Res Int 2014:596498
15. Pile J and Simaan N (2013) Characterization of friction and speed effects and methods for detection of cochlear implant electrode tip fold-over. In: 2013 IEEE International Conference on Robotics and Automation, pp 4409–4414
16. Meshik X, Holden TA, Chole RA, Hullar TE (2010) Optimal cochlear implant insertion vectors. Otol Neurotol 31(1):58–63

17. Cochlear™ Nucleus® CI632 cochlear implant with Slim Modiolar electrode, Physician's Guide, Cochlear™, Canada https://www.cochlear.com/ifu/documents/d1144283-en-ci632
18. O'Connell BP, Hunter JB, Wanna GB (2016) The importance of electrode location in cochlear implantation. Laryngoscope Investig Otolaryngol 1(6):169–174
19. Zuniga MG, Böttcher G, Schell V, Lenarz T, Rau TS (2021) Illustrating orientation changes of the insertion trajectory during cochlear implant electrode array insertion. Curr Direct Biomed Eng 7(2):113–116
20. Jia H, Pan J, Gu W, Tan H, Chen Y, Zhang Z, Jiang M, Li Y, Sterkers O, Wu H (2021) Robot-Assisted electrode array insertion becomes available in pediatric cochlear implant recipients: first report and an intra-individual study. Front Surg 8:695728
21. Torres R, Jia H, Drouillard M, Bensimon JL, Sterkers O, Ferrary E, Nguyen Y (2018) An optimized robot-based technique for cochlear implantation to reduce array insertion trauma. Otolaryngol Head Neck Surg 159(5):900–907
22. Torres R, Daoudi H, Lahlou G, Sterkers O, Ferrary E, Mosnier I, Nguyen Y (2021) Restoration of high frequency auditory perception after robot-assisted or manual cochlear implantation in profoundly deaf adults improves speech recognition. Front Surg. https://doi.org/10.3389/fsurg.2021.729736

IV.

Új műtéti képalkotó lehetőség a belsőfül-implantátum elektródasorának dinamikus helyzetmeghatározására

Perényi Ádám dr.* ▪ Nagy Roland dr.* ▪ Horváth Bence ▪ Posta Bálint dr. Dimák Balázs ▪ Csanády Miklós dr. ▪ Kiss József Géza dr. ▪ Rovó László dr.

Szegedi Tudományegyetem, Általános Orvostudományi Kar, Fül-Orr-Gégészeti és Fej-Nyaksebészeti Klinika, Szeged

Bevezetés: A cochlearis implantátum egy műtétileg behelyezett elektromos eszköz, amely az akusztikus hanghullámokat elektromos jelekké alakítja, közvetlenül a hallóideget stimulálja, így segíti a súlyos fokú hallássérüléssel vagy teljes hallásvesztéssel élők életét. Cochlearis implantációt követően a legjobb rehabilitációs eredmény elérésének technikai feltétele többek között az esetre szabott elektródaválasztás és az elektródasor teljes, kontrollált, szövődménymentes bejuttatása a scala tympaniba, miközben a cochlea belső struktúrája a lehető legkisebb mértékben sérül. A rutin intraoperatív elektrofiziológiai tesztek fontos információt adnak a készülék működőképességéről és a hallóideg stimulációjáról, azonban nem hagyatkozhatunk rájuk az elektródasor cochleán belüli helyzetének igazolásában. Mivel előfordulhat, hogy a rendelkezésre álló elektrofiziológiai vizsgálatok eredménye megfelelő, és mégis rendellenes helyzetbe kerül az elektróda, az arany standardot a képalkotó vizsgálatok jelentik.
Módszer: Közleményünkben egy modern, hibrid műtő által nyújtott technológiai háttér új alkalmazási területét mutatjuk be. Szimultán kétoldali cochlearis implantációt végeztünk Cochlear Nucleus Slim Modiolar típusú perimodiolaris elektródasorral, a belső fül fejlődési rendellenességével rendelkező betegen. Az intraoperatív képalkotást Siemens Artis pheno C-karos robot digitális szubtrakciós angiográfiás rendszer biztosította valós idejű átvilágító és volumentomográfiás funkcióval.
Eredmények: Az intraoperatív képalkotás által dinamikusan követhető az elektródasor bevezetésének folyamata, ellenőrizhető az elektródasor statikus helyzete, így kiváltható a rutinnak számító posztoperatív képalkotó vizsgálat. A rendellenes helyzetbe kerülő elektródasor pozíciója egy ülésben korrigálható, az újból bevezethető, így elkerülhető az újabb altatással járó, bizonytalan kimenetelű revíziós műtét.
Következtetés: A hibrid műtő jól kontrollált, minimálisan invazív eljárások elvégzését biztosítja. Különösen a hallószerv fejlődési rendellenessége vagy egyéb, az elektródának a cochleába vezetését nehezítő rendellenesség esetén javasolt a műtői képalkotó diagnosztika.
Orv Hetil. 2021; 162(22): 878–883.

Kulcsszavak: cochlearis implantátum, Slim Modiolar elektródasor, cochlearis malformatio, hibrid műtő, intraoperatív képalkotás

A novel intraoperative imaging tool to follow the cochlear implant electrode array insertion dynamics

Introduction: The cochlear implant is a surgically inserted electrical device that converts acoustic sound waves into electrical signals to stimulate the cochlear nerve, thus helps the rehabilitation of people with severe to total hearing loss. One of the most important technical conditions for achieving the best rehabilitation result after cochlear implantation is the personalized choice of electrodes. Additionally, it is vital that there is a complete, controlled, uncomplicated delivery of the electrode array to the scala tympani while minimizing damage to the inner structures of the cochlea. Routine electrophysiological tests provide important information about device functionality and auditory nerve stimulation. However, they probably do not show an abnormal position of the electrode array within the cochlea. Thus, imaging studies remain the gold standard.

*Megosztott első szerzők.

Method: In our paper, we present a novel application field of the modern technological background provided by a hybrid operating room. Simultaneous bilateral cochlear implantation was performed with cochlear implants with perimodiolar electrode array (Nucleus Slim Modiolar) in a patient with cochlear malformation. Intraoperative imaging was provided by a Siemens Artis pheno C-arm robot digital subtraction angiography system with real-time fluoroscopy and volume tomography function.
Results: Intraoperative imaging ensures dynamic follow-up of the introduction and static determination of the position of the electrode array and replaces routine postoperative imaging. If the electrode array was inserted in an abnormal position, the revision can be performed in the same sitting. Also, the revision surgery with a potential risk of uncertain outcome, alongside additional anaesthesia, can be prevented.
Conclusion: The hybrid operating room ensures that well-controlled, minimally invasive procedures are performed. Intraoperative imaging can be imperative in malformed cochleae and conditions that may complicate electrode insertion.

Keywords: cochlear implant, Slim Modiolar electrode array, cochlear malformation, hybrid operating room, intraoperative imaging

Perényi Á, Nagy R, Horváth B, Posta B, Dimák B, Csanády M, Kiss JG, Rovó L. [A novel intraoperative imaging tool to follow the cochlear implant electrode array insertion dynamics]. Orv Hetil. 2021; 162(22): 878–883.

(Beérkezett: 2020. október 16.; elfogadva: 2020. november 27.)

Rövidítések

CT = (computed tomography) komputertomográfia; DSA = (digital subtraction angiography) digitális szubtrakciós angiográfia; ESRT = (electrical evoked stapedius reflex threshold) az elektromosan kiváltott stapedius reflex küszöbe; MR = (magnetic resonance) mágneses rezonancia; NRT = (neural response telemetry) idegiválasz-telemetria

Cochlearis implantáció során a megfelelő elektródasor pozicionálása kihívást jelenthet olyan esetekben, mint a belső fül fejlődési rendellenessége vagy a hallószerv részleges hiánya, kötőszövetes átalakulása vagy elcsontosodása. Az esetek nagy többségében az ilyen rendellenességek műtétet megelőzően azonosíthatók szeletelő képalkotó eljárásokkal (CT- és/vagy MR-vizsgálattal).

Az ezen esetek adta behelyezési nehézségek felismerése befolyásolhatja a sebészt a beültetett eszköz (elektródasor) kiválasztásában, vagy módosítást igényelhet a műtéti megközelítés.

Szövődmények még kellő elővigyázatosság és gondosság mellett is kialakulhatnak. Az elektródasornak a cochleába történő bevezetését követően szembesülhetünk azzal, hogy rendellenes helyzetbe került. Ilyen rendellenes pozíció lehet a részleges bevezetés, a megtöretés, a felgyűrődés vagy akár visszatekeredés (*1. ábra)* és az egyensúlyszervbe kerülés [1–3]. Számos publikáció szerzői beszámoltak már az elektródasor behelyezése során az ún. interscalaris diszlokációról, ami azt jelenti, hogy az elektródasor átszakítja az alapi hártyát, és így a scala tympaniból részben a scala vestibuliba kerül át [1, 4, 5]. Ismerünk olyan eseteket is, amelyeknél évekkel a műtét után az elektródasor migrált a cochleán kívülre [1, 5, 6].

Klinikai protokollunkban a cochlearis implantáció során alkalmazott általános vizsgálati módszereink az impedanciavizsgálat, az elektromosan kiváltott stapediusreflex küszöbének (electrical evoked stapedius reflex threshold, ESRT) mérése és az idegiválasz-telemetria (neural response telemetry, NRT). Ezek a mérési módszerek nem jelzik egyértelműen az elektródasor rendellenes bevezetését, hanem az elektródasor állapotáról (szakadás, sérülés), környezetének elektromos vezetőképességéről és a közölt elektromos jel által stimulált idegelemekben kiváltható akciós potenciál jelenlétéről adnak információt. A legtöbb, cochlearis implantációt végző központ számára műtéti képalkotó vizsgálat nem áll rendelkezésre, ezért általában a műtét másnapján végeznek képalkotó vizsgálatot, ami lehet röntgenfelvétel, ’cone-beam’ (kúpsugaras) CT- vagy hagyományos (multi slide) CT-vizsgálat [7].

Amennyiben az elektróda bevezetését követően azonnal felismerjük az elektródasor rendellenes helyzetét, még ugyanabban az ülésben megtörténhet a repozicionálás. Intraoperatív képalkotásra alkalmas készülékek a mobil röntgen, az átvilágító, a fekvő ’cone-beam’ CT- és a DSA-készülék. Ha azonban intraoperatív képalkotásra – mint a világ legtöbb, implantációt végző fülészeti műtőjében – egyelőre nincs mód, akkor a korrekció újabb műtétet jelent. Ezért az intraoperatív képalkotás lehetősége és szerepe felértékelődik, és így egy ülésben elvégezhető az elektróda reimplantációja [3, 8–11]. Különösen fontos az elektródasor típusának helyes megválasztása és pozíciójának ellenőrzése a cochlea fejlődési rendellenességei [12] esetében.

A kontrollált, szövődménymentes implantációt nagymértékben elősegíti a modern technológiai háttér. Ezen technológiák készségszintű használata, a pontosan összehangolt csapatmunka hatékonysága biztosítja a gyors és eredményes beavatkozások számát. Erre alkalmas, igen effektív közeg lehet a hibrid műtő, mely a hallásja-

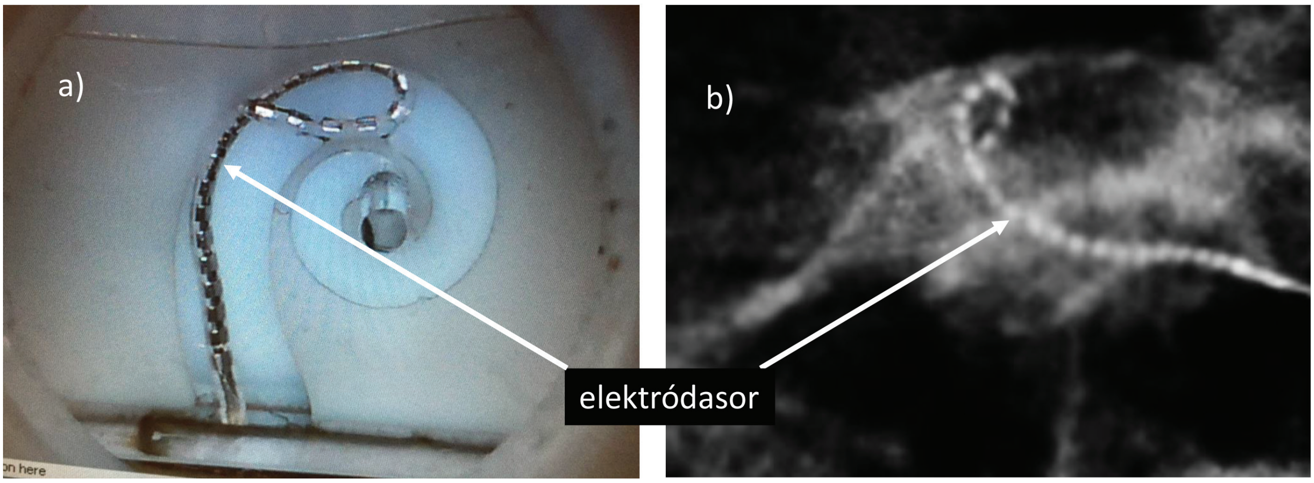

1. ábra | A Slim Modiolar elektródasor cochleán belüli visszatekeredése gyakorló modellen (1/a) és posztoperatívan készített röntgenfelvételen (1/b). A modellen az 5. elektródánál, a röntgenfelvételen a 4. elektródánál látható az elektródasor csúcsi szakaszának cochleán belüli visszatekeredése

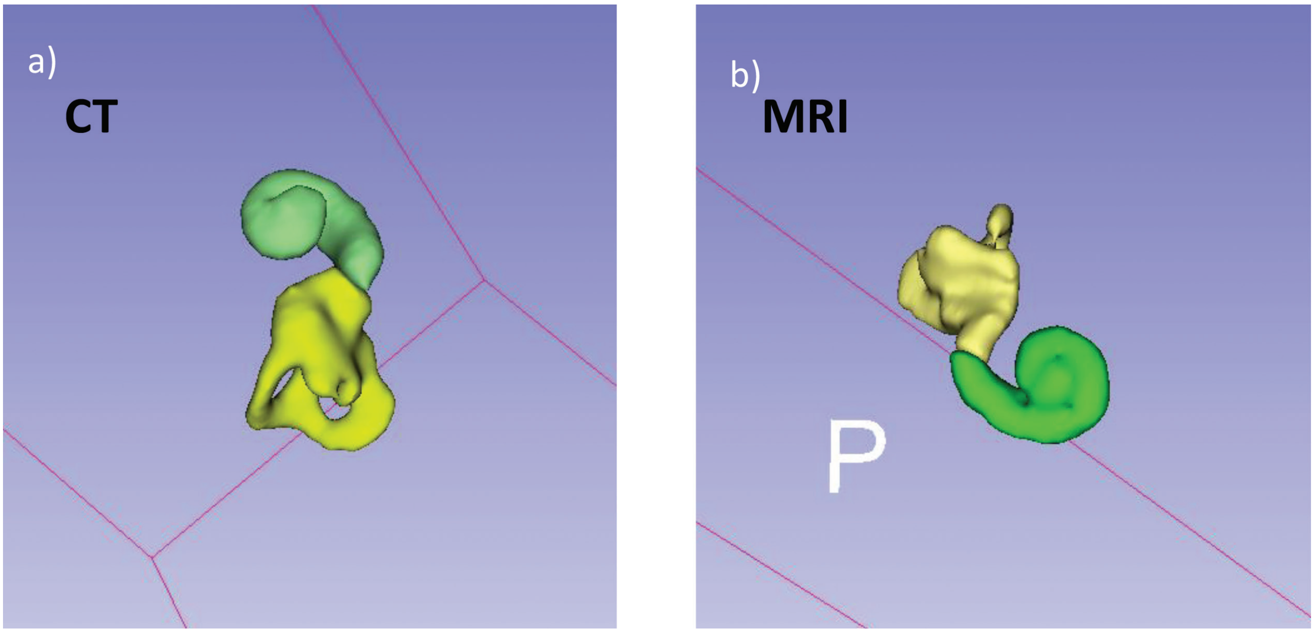

2. ábra | Az 1 éves páciensünk jobb oldali labyrinthusának belső, folyadéktartalmú részéről készített háromdimenziós rekonstrukciós képek, a körülötte lévő csontállomány ábrázolása nélkül; CT alapján (2/a) és MRI alapján (2/b). A cochlea átlagos méretű alapi kanyarulatát követően a második kanyarulat csökevényes, mindössze fél fordulatot tesz, és hiányzik a harmadik kanyarulat

CT = komputertomográfia; MRI = mágnesesrezonancia-képalkotás

vító implantáció esetében nemzetközi viszonylatban nem elterjedt módszer. A hibrid műtő egy fejlett operációs tér, amely ötvözi a hagyományos műtőt egy képalkotók által vezérelt intervenciós csomaggal. Ez a kombináció rendkívül összetett, fejlett műtéti eljárásokat tesz lehetővé. Nemcsak a műtőtípusokat kombinálja, hanem csapatok is egyesülnek, és multidiszciplináris klinikusi csoportot alkotnak, felkészülve a betegek összetett igényeinek kielégítésére. Bár a képalkotás hosszú ideje a standard műtők része lehet, a mobil C-karos átvilágító készülék, ultrahang vagy endoszkóp jelenlétével, ezek együttes használata és megfelelő technikai háttere a hibrid műtők jellegzetessége.

Anyag és módszer

Páciensünk 1 éves, kétoldali teljes hallásvesztéssel élő fiúgyermek, akinek a kivizsgálás részeként elvégzett CT- és MR-vizsgálataival mindkét belső fül malformatiója volt kimutatható. A gyermek mindkét cochleájának ún. III. típusú cochlearis hypoplasiáját azonosítottuk a Sennaroğlu-féle besorolás [12] szerint. Ez az elváltozás azt jelenti, hogy a cochlea átlagos méretű alapi kanyarulatát követően a második kanyarulat csökevényes, mindössze fél fordulatot tesz, és hiányzik a harmadik kanyarulat. A cochlea belső szerkezete (scala tympani, media és vestibuli) megtartott. Ez a cochleamalformatio társulhat az egyensúlyszerv fejlődési rendellenességével, így esetünkben a lateralis ívjáratok részleges hiányával *(2. ábra)*.

A két fül cochlearis implantációját egy ülésben, 2020-ban, a Szegedi Tudományegyetem Szent-Györgyi Albert Klinikai Központjának hibrid műtőjében végeztük el, Cochlear Nucleus CI632 típusú, perimodiolaris tulajdonságú elektródasorral rendelkező implantátummal (Cochlear Ltd., Sydney, Ausztrália). Az intraoperatív képalkotást Siemens Artis pheno (Siemens Healthcare GmbH, Erlangen, Németország) robot DSA-rendszer biztosította.

A cochlearis implantációhoz a legelterjedtebb műtéti módszert alkalmaztuk: retroauricularis feltárást követően részleges mastoidectomiát végeztünk, majd vigyázva az arcidegre, posterior tympanotomiás nyílást készítettünk. Az elektródasort ezen keresztül bejuttatva a dobüregbe, a cochlea kerek ablakán keresztül teljesen bevezettük a cochlea scala tympani járatába. A rutin elektrofiziológiai mérési protokollt (impedancia, ESRT, NRT) követtük.

Eredmények

Az elektródasor cochleába történő bevezetésének folyamatát a C-karos DSA-készülék segítségével, az átvilágító funkcióval követtük külön-külön a két oldalon *(3. és 4. ábra)*.

Az elektródasor bevezetésekor az operáló fülsebész nem érzékelt akadályozó tényezőt, és az intraoperatíven elvégzett rutin elektrofiziológiai mérések az implantátumok működőképességét igazolták. A második implantátum beültetését követően ugyanazzal a C-karos DSA-készülékkel rétegfelvételeket készítettünk a koponyáról *(5. ábra)*.

Az implantátumhoz tartozó külső beszédprocesszorok első programozásakor – amelyet a műtétet követő negyedik héten végeztünk – a gyermeknél egyértelmű hallásélményt tapasztaltunk. Az implantátum 22 stimulálóponttal rendelkezik, melyek segítségével meghatároztuk a gyermek elektromos komfortküszöbét. Az elektromos komfortküszöb az a legmagasabb áramintenzitás-érték, amely a hallópálya intenzív stimulálását jelenti, de még nem kelt kellemetlen, túl hangos érzést. A gyermek mindkét oldalon, minden elektróda esetében érdeklődéssel figyelt a hangként érzékelt elektromos jelekre.

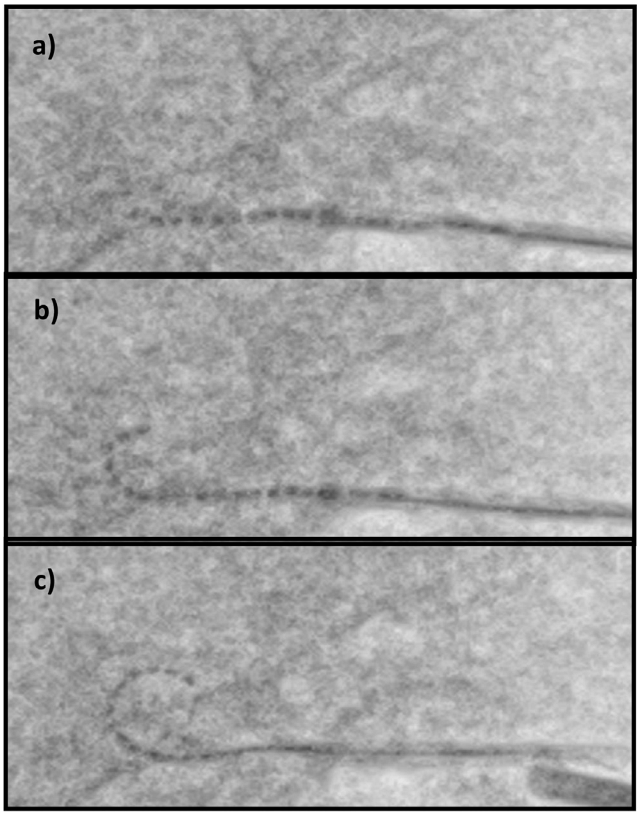

4. ábra C-karos DSA-készülék segítségével valós idejű átvilágító képsor készíthető az elektródasor bevezetéséről. Az elektródasor vége a cochlea basalis kanyarulatának medialis caudalis részében (4/a), cranialis részében (4/b) és a teljes bevezetés állapotában (4/c)

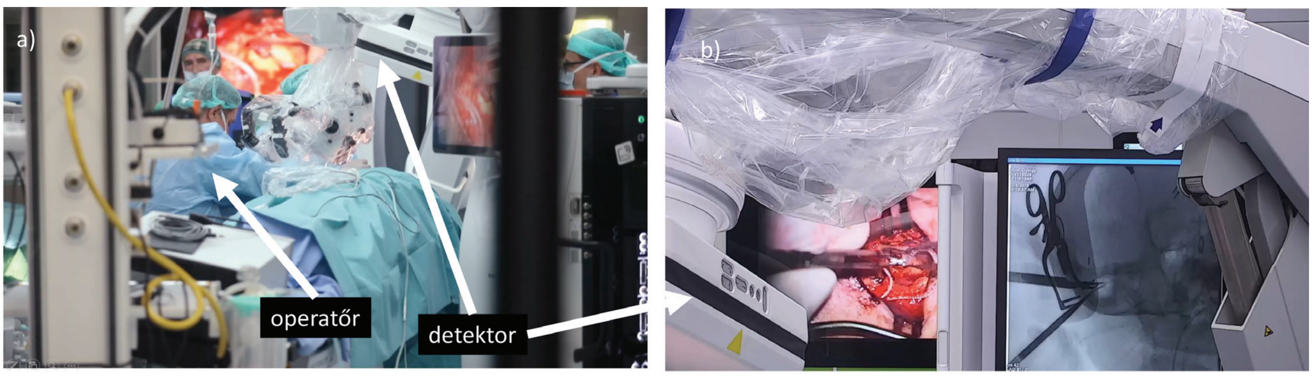

3. ábra Műtői helyzetkép. A C-karos DSA-készülék helyzete a műtőasztalhoz és az operatőrhöz képest (3/a ábra). A 3/b ábra bal oldalán, a C-karos DSA-készülék 'flat panel' detektorának takarásában lévő monitoron a mikroszkópról kivezetett műtéti kép, a jobb oldalán lévő monitoron a valós idejű átvilágító kép látható, az elektróda bevezetésekor

DSA = digitális szubtrakciós angiográfia

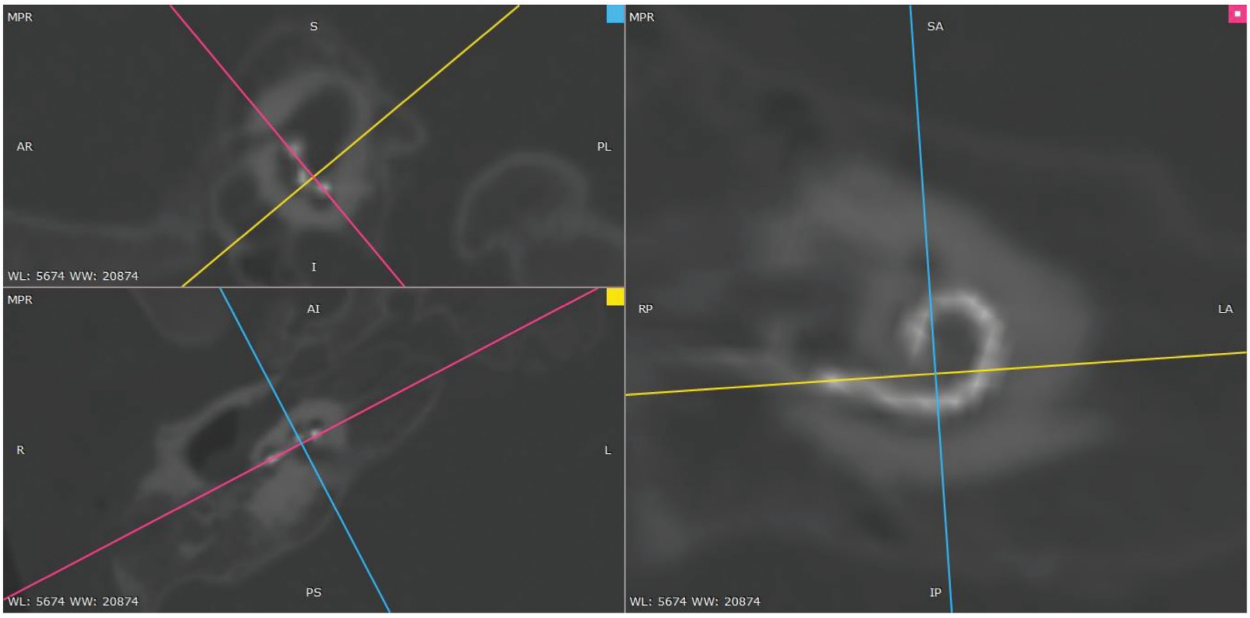

5. ábra A Siemens Artis pheno készülékkel készített, több síkban rekonstruált volumentomográfiás felvétel. A jobb oldali képen az ún. cochlearis nézetet mutatjuk be a cochlea alapi kanyarulatáról, benne a teljesen bevezetett és perimodiolaris helyzetű elektródasorral

A későbbiekben havi rendszerességgel jelent meg hozzátartozóival állapotellenőrzésre, melyeken újabb beszédprocesszor-programozás történt az elektromos komfortküszöb változásának követésére. Édesanyja hónapról hónapra újabb eredményeket osztott meg: kezdetben a gyermek felfigyelt a külső zajokra, a beszédhangokra, majd az egyszerű utasításokra. A műtétet követő kilencedik hónapra a ritmika nélküli gügyögést tudatos, egyszerű hangformálás váltotta fel. A gyermek környezetében jelen lévő hangok, a szülők és a fejlesztőpedagógus által tanított hangok utánzását meghatározó eredményként könyvelhetjük el a beszédfejlődésének útján. A hallás mellett a gyermek mozgáskoordinációja is jelentősen fejlődött.

Megbeszélés

A cochlearis implantáció követelménye az inszerciós trauma minimalizálása mellett a minél jobb beszédértés lehetőségének biztosítását lehetővé tevő, elektródasorral felszerelt implantátum beültetése [13, 14]. A vékony perimodiolaris elektróda ötvözi ezen előnyöket, ugyanakkor bevezetésekor más elektródatípusokhoz képest gyakoribb jelenség az elektródasor csúcsi részének cochleán belüli visszacsavarodása [1, 3, 9–11, 13]. Amennyiben ez a szövődmény még sebzárás előtt észlelésre kerül, jó eséllyel korrigálható ugyanabban az ülésben. A közleményünkben bemutatott módszer – az elektródasor bevezetésekor végzett átvilágítás – valós időben képes követni az elektródasor útját és helyzetét a cochleán belül. A cochlea funkcionális rendszerét tartalmazó hártyás labyrinthust kompakt csontállomány veszi körül, ezért vizuálisan nem tudjuk követni az operációs mikroszkóppal az elektróda útját. A rendelkezésre álló rutin elektrofiziológiai vizsgálatokkal nem ismerhető fel biztonsággal az elektródasor rendellenes helyzete, és az operáló sebész sem érzékeli azt. A valós idejű képalkotó vizsgálattal azonnal felismerhető, ha az elektródasor a modiolustól eltávolodik, visszacsavarodik, megtörik vagy az egyensúlyszervbe kerül. Az elektródasort kissé visszahúzva vagy teljesen eltávolítva – az elektródasor típusától függően – az jó eséllyel korrigálható és jó pozícióba helyezhető vissza. A III. típusú cochleahypoplasiás esetünkben a basalis kanyarulat átlagos nagyságú, megtartott volt. Cochlearis hypoplasia malformatióban a rövid egyenes elektródasor beültetését ajánlják [12]. Esetünkben azért választottuk a vékony, előgörbített elektródát, mert 1 éves páciensünknél fontosnak tartottuk a beszédfejlődés szempontjából az elektródasor modiolushoz közeli helyzetét és a cochlea szerkezetében okozott trauma minimalizálását.

A Szegedi Tudományegyetem Szent-Györgyi Albert Klinikai Központjában működő hibrid műtő a legmodernebb képalkotó készülékkel felszerelt egység. A Siemens Artis pheno C-karos robot DSA-készülék egyesíti a mobil röntgen, az átvilágító és a ’cone-beam’ CT-készülékek előnyeit: nagy teljesítményű, gyors, minden irányba jól pozicionálható sugárforrással és ’flat panel’ detektorral rendelkezik, ami lehetővé teszi, hogy az elektróda bevezetését a cochleába valós időben követhessük átvilágítással, nagy felbontású monitoron. Emellett volumentomográfia is készíthető vele, amely a ’cone-beam’ CT-nek megfelelő, nagy felbontású képeket biztosít alacsony sugárdózissal és kevés fém műtermékkel [15]. Esetünkben az átvilágítás módszerével rendellenességet nem tapasztaltunk. Az elektróda bevezetését követően elvégzett, alacsony sugárdózisú volumentomográfia alapján igazoltuk, hogy az elektródasor teljesen bevezethető volt, és a modiolushoz közel került.

Következtetés

A hibrid műtő aszeptikus környezete egyesíti a sebészeti berendezéseket, műszereket, műtéti asztalokat, operációs lámpákat, berendezést kezelő rendszereket a karokra rögzített fejlett képalkotó rendszerekkel együtt, és lehetőséget kínál kombinált képalkotással vezérelt eljárások végrehajtására, minimálisan invazív módszerekkel. Ezek a korszerű műtőszobák lehetővé teszik a képalkotás-vezérelt műtét és a nyitott feltárások kombinációját is. Ez a technológia új eljárások kifejlesztéséhez vezetett, amelyek előnyös lehetőségeket kínálnak a komplex betegségben szenvedő páciensek számára [16–18].

A cochlearis implantációs centrumok számára ajánljuk az intraoperatív képalkotás bevezetését jól kontrollált, minimálisan invazív eljárások biztosítására. A C-karos röntgenátvilágító berendezések fejlesztőitől új innovációs eredményekre számítunk a készülékek rutinszerű, könnyű használatában, akár külön a fej-nyak sebészet igényeinek megfelelően. Az intraoperatív képalkotás kiváltja a rutinszerűen az első posztoperatív napon több nézetben végzett röntgenvizsgálatot, mely az életkorból adódóan nem együttműködő gyermekek esetében a mozgási műtermékek miatt korlátozottan értékelhető lehet, és a vizsgálat megismétlését teheti szükségessé.

Ezen korszerű módszerek protokollszerű alkalmazásával a rendellenes helyzetbe kerülő elektródasor korrekciója egy ülésben elvégezhető, így kiváltható a műtétet követő röntgenvizsgálat, elkerülhető az újabb altatással és műtéti megterheléssel járó revízió.

Anyagi támogatás: A közlemény megírása, illetve a kapcsolódó kutatómunka anyagi támogatásban nem részesült.

Szerzői munkamegosztás: P. Á. és N. R. megosztott első szerzőként jegyzik a kéziratot. P. Á.: Az ábrák megszerkesztése, az intraoperatív képalkotás kivitelezése, a kézirat szövegezése. N. R.: Az ábrák megszerkesztése, az elektrofiziológiai vizsgálatok elvégzése, a kézirat szövegezése. H. B.: A képalkotó vizsgálatok rekonstrukciójának elkészítése és az intraoperatív képalkotás kivitelezése. P. B.: A szakirodalom áttekintése, a kézirat véglegesítése. D. B.: A szakirodalom áttekintése, elektrofiziológiai mérések elvégzése. Cs. M.: A kézirat szakmai véleményezése és a publikációra való felkészítése. K. J. G.: Az elektrofiziológiai mérések ellenőrzése, az eredmények értékelése; tudományos tanácsadás. R. L.: Az implantációs team vezetője; a cochlearis implantáció elvégzése, a végleges kézirat véleményezése, a publikáció folyamatának követése, irányítása. A cikk végleges változatát valamennyi szerző elolvasta és jóváhagyta.

Érdekeltségek: A szerzőknek nincsenek érdekeltségeik.

Irodalom

[1] Ishiyama A, Risi F, Boyd P. Potential insertion complications with cochlear implant electrodes. Cochlear Implants Int. 2020; 21: 206–219.
[2] Adunka O, Kiefer J. Impact of electrode insertion depth on intracochlear trauma. Otolaryngol Head Neck Surg. 2006; 135: 374–382.
[3] Zuniga MG, Rivas A, Hedley-Williams A, et al. Tip fold-over in cochlear implantation: case series. Otol Neurotol. 2017; 38: 199–206.
[4] Saeed SR, Selvadurai D, Beale T, et al. The use of cone-beam computed tomography to determine cochlear implant electrode position in human temporal bones. Otol Neurotol. 2014; 35: 1338–1344.
[5] Dietz A, Wennström M, Lehtimäki A, et al. Electrode migration after cochlear implant surgery: more common than expected? Eur Arch Otorhinolaryngol. 2016; 273: 1411–1418.
[6] Rader T, Baumann U, Stöver T, et al. Management of cochlear implant electrode migration. Otol Neurotol. 2016; 37: e341–e348.
[7] Ramos de Miguel Á, Argudo AA, Borkoski Barreiro SA, et al. Imaging evaluation of electrode placement and effect on electrode discrimination on different cochlear implant electrode arrays. Eur Arch Otorhinolaryngol. 2018; 275: 1385–1394.
[8] Ramos-Macias A, De Miguel AR, Falcon-González JC. Mechanisms of electrode fold-over in cochlear implant surgery when using a flexible and slim perimodiolar electrode array. Acta Otolaryngol. 2017; 137: 1129–1135.
[9] Aschendorff A, Briggs R, Brademann G, et al. Clinical investigation of the nucleus slim modiolar electrode. Audiol Neurootol. 2017; 22: 169–179.
[10] Sabban D, Parodi M, Blanchard M, et al. Intra-cochlear electrode tip fold-over. Cochlear Implants Int. 2018; 19: 225–229.
[11] McJunkin JL, Durakovic N, Herzog J, et al. Early outcomes with a slim, modiolar cochlear implant electrode array. Otol Neurotol. 2018; 39: e28–e33.
[12] Sennaroğlu L, Bajin MD. Classification and current management of inner ear malformations. Balkan Med J. 2017; 34: 397–411.
[13] Schieferbein V, Bredemann J, Schmitt R, et al. Influence of patient-specific anatomy on medical computed tomography and risk evaluation of minimally invasive surgery at the otobasis. Eur Arch Otorhinolaryngol. 2019; 276: 375–382.
[14] Nagy R, Jarabin JA, Dimák B, et al. Possibilities for residual hearing preservation with Nucleu CI532 Slim Modiolar electrode array. [A maradványhallás megőrzésének lehetőségei cochlearis implantáció során Nucleus CI532 Slim Modiolar elektródasorral.] Orv Hetil. 2018; 159: 1680–1688. [Hungarian]
[15] Perényi Á, Bella Z, Baráth Z, et al. Role of cone-beam computed tomography in diagnostic otorhinolaryngological imaging. [A cone-beam komputertomográfia alkalmazása a fül-orr-gégészeti képalkotásban.] Orv Hetil. 2016; 157: 52–58. [Hungarian]
[16] Nollert G, Wich S. Planning a cardiovascular hybrid operating room: the technical point of view. Heart Surg Forum 2009; 12: E125–E130.
[17] Schaadt J, Landau B. Hybrid OR 101: A primer for the OR nurse. AORN J. 2013; 97: 81–100.
[18] Fuchs-Buder T, Settembre N, Schmartz D. Hybrid operating theater. [Hybridoperationssaal.] Anaesthesist 2018; 67: 480–487. [German]

(Perényi Ádám dr.,
Szeged, Tisza Lajos krt. 111., 6725
e-mail: perenyi.adam@med.u-szeged.hu)